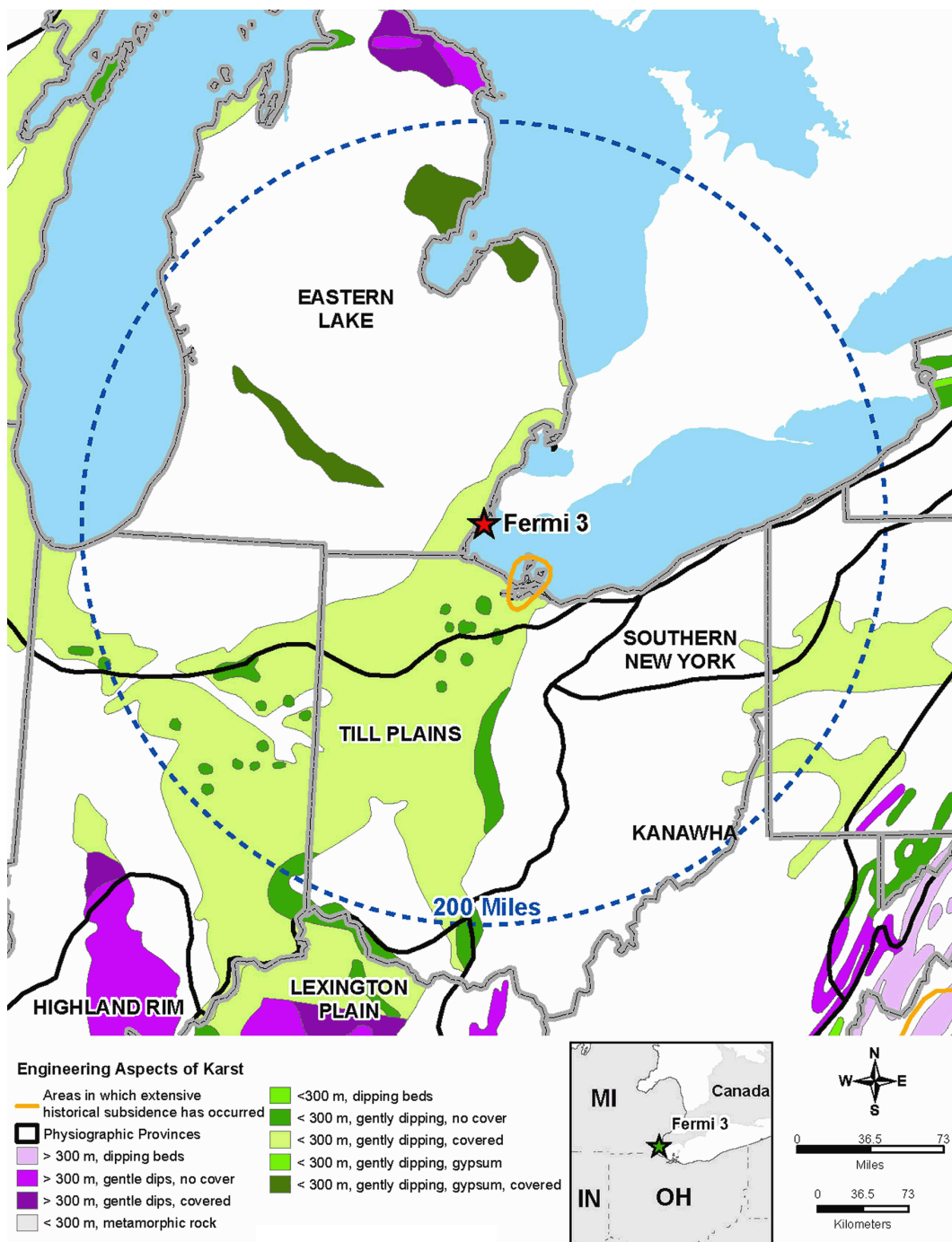


Figure 2.5.1-228 Engineering Aspects of Karst Map for the Fermi 3 Site Region



Source: Reference 2.5.1-388

Figure 2.5.1-229 Topography of the Fermi 3 Site Location

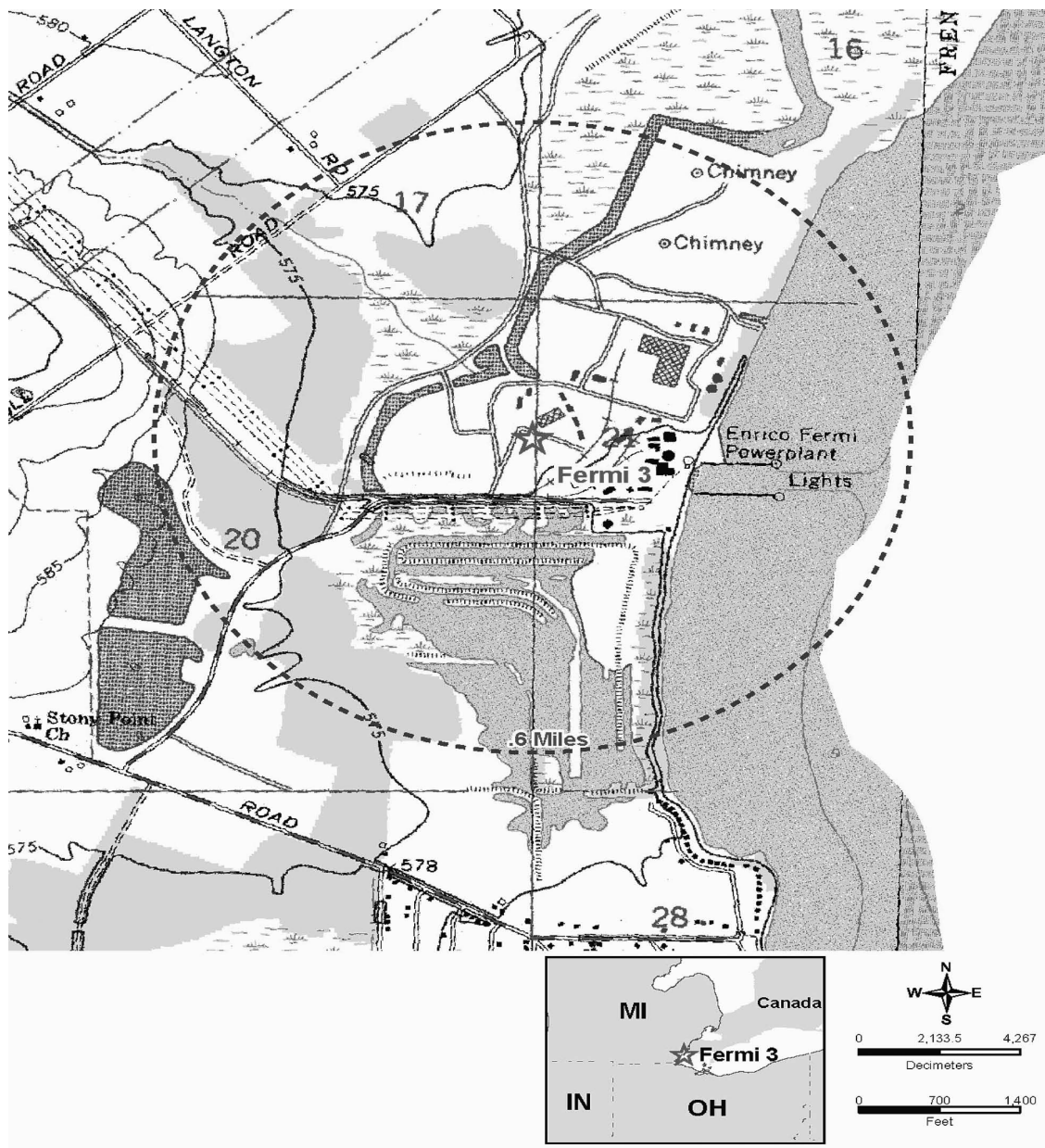


Figure 2.5.1-230 Geologic Map of the Fermi 3 Site Vicinity

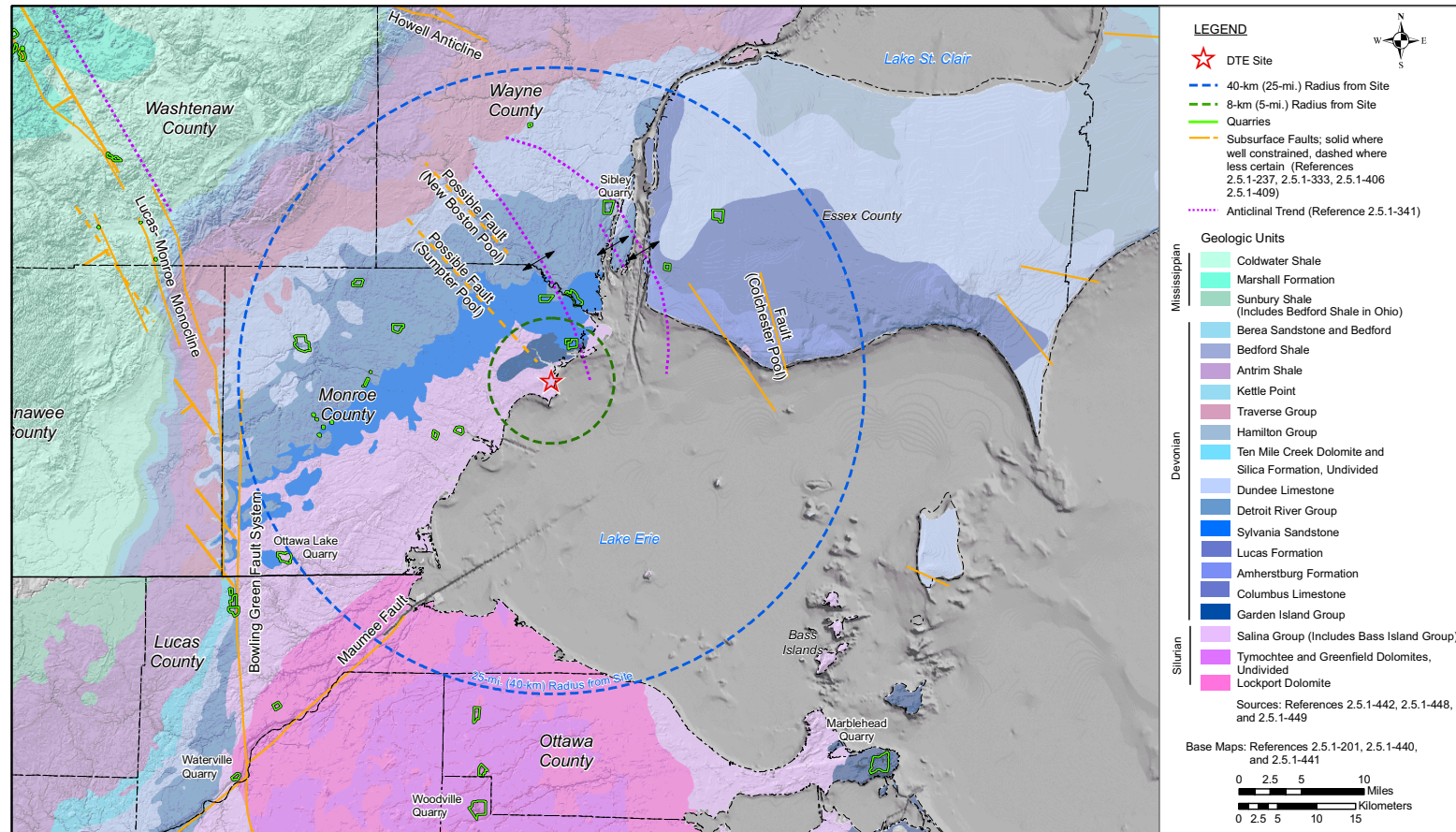


Figure 2.5.1-231 Geologic Map Showing Quaternary Features of the Fermi 3 Site Vicinity

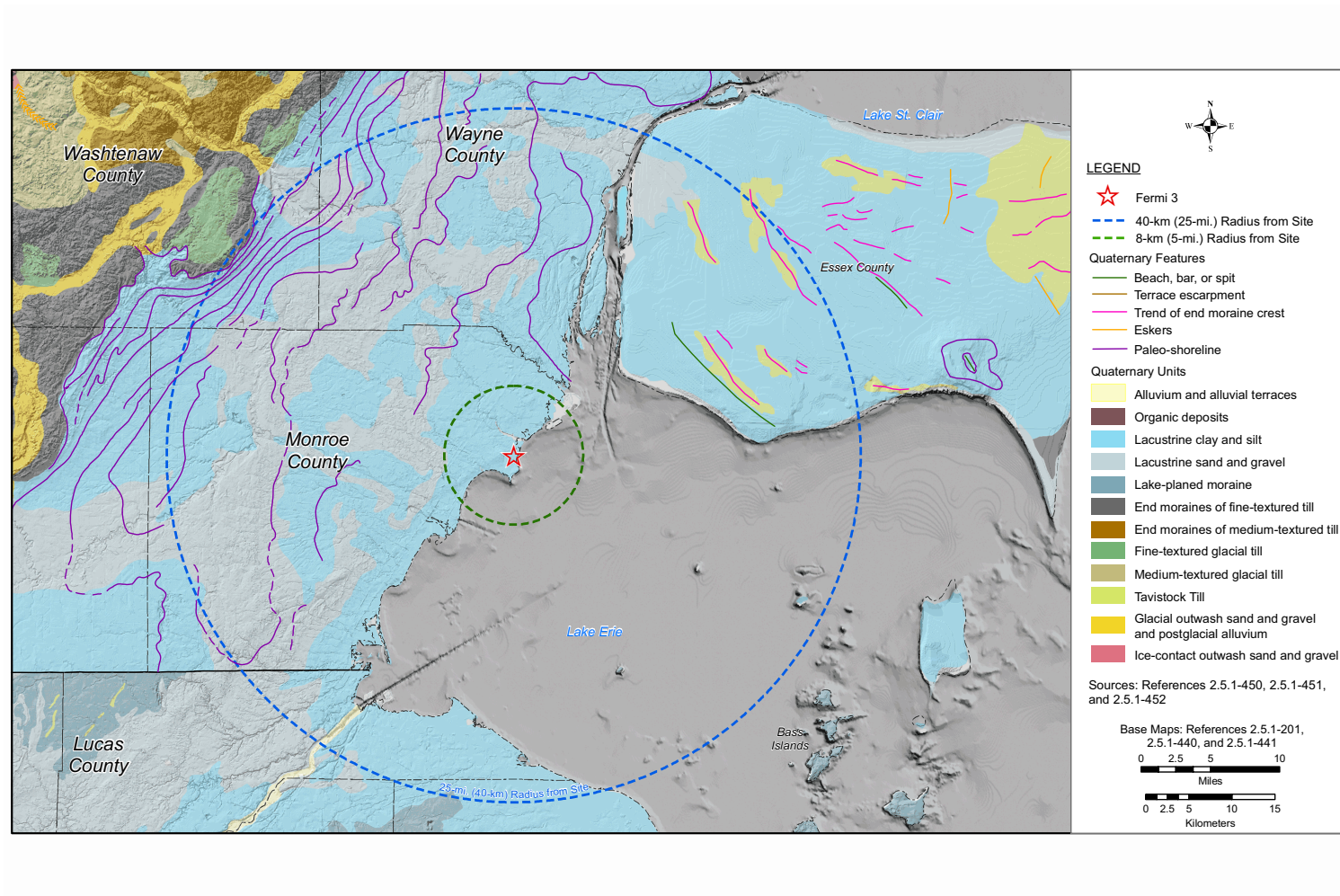
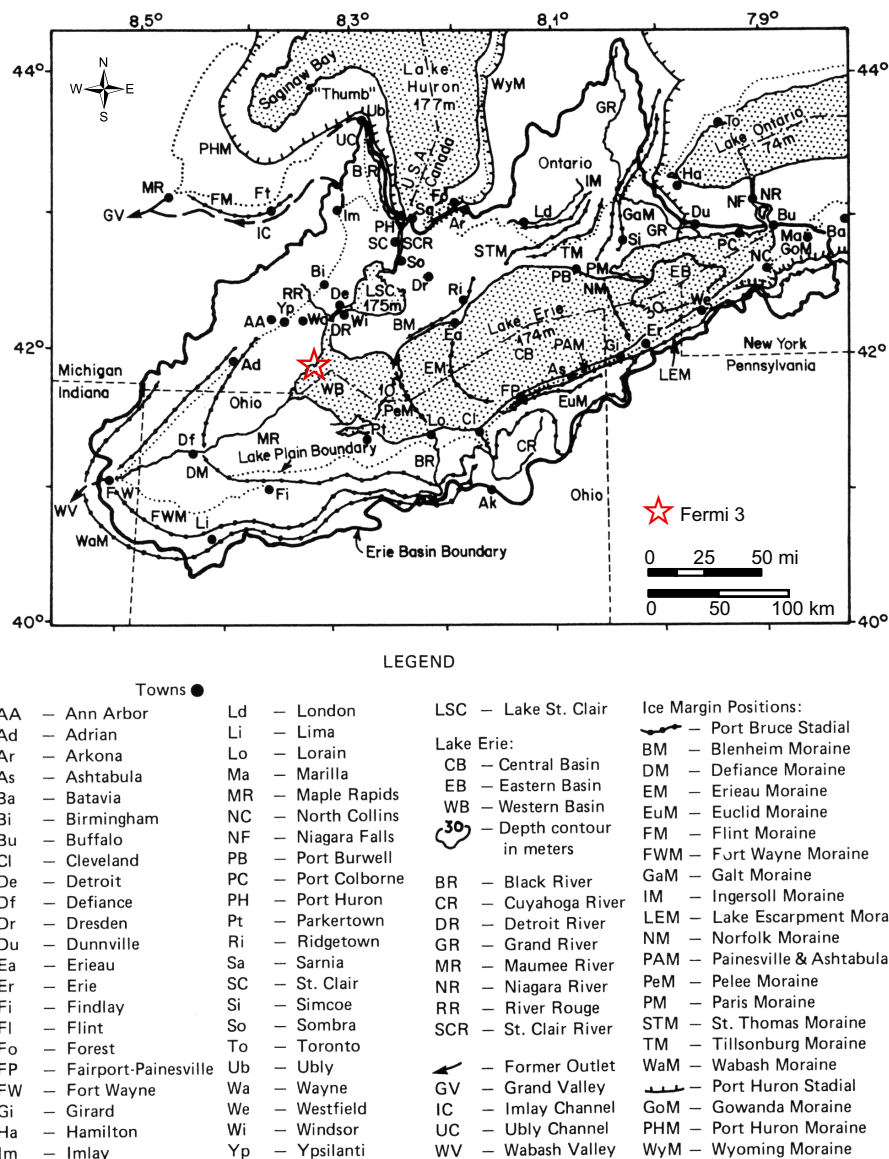
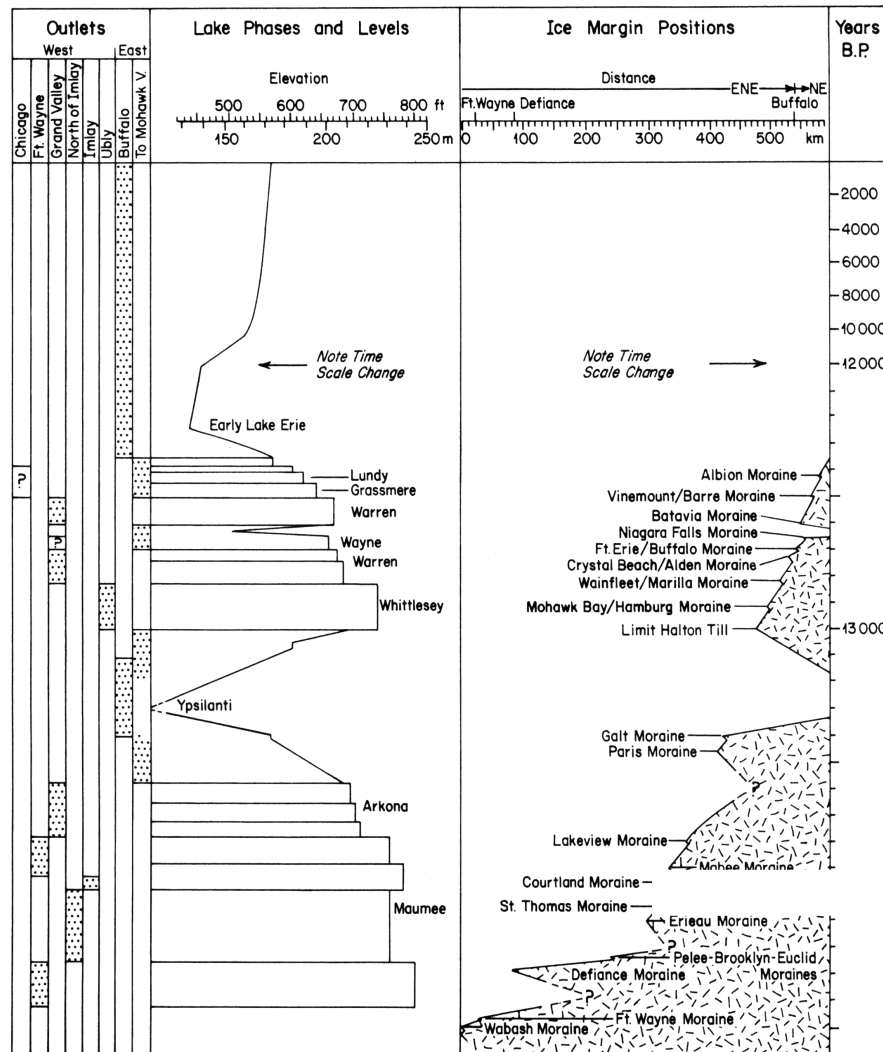


Figure 2.5.1-232 Map Showing Quaternary Features of the Erie Basin



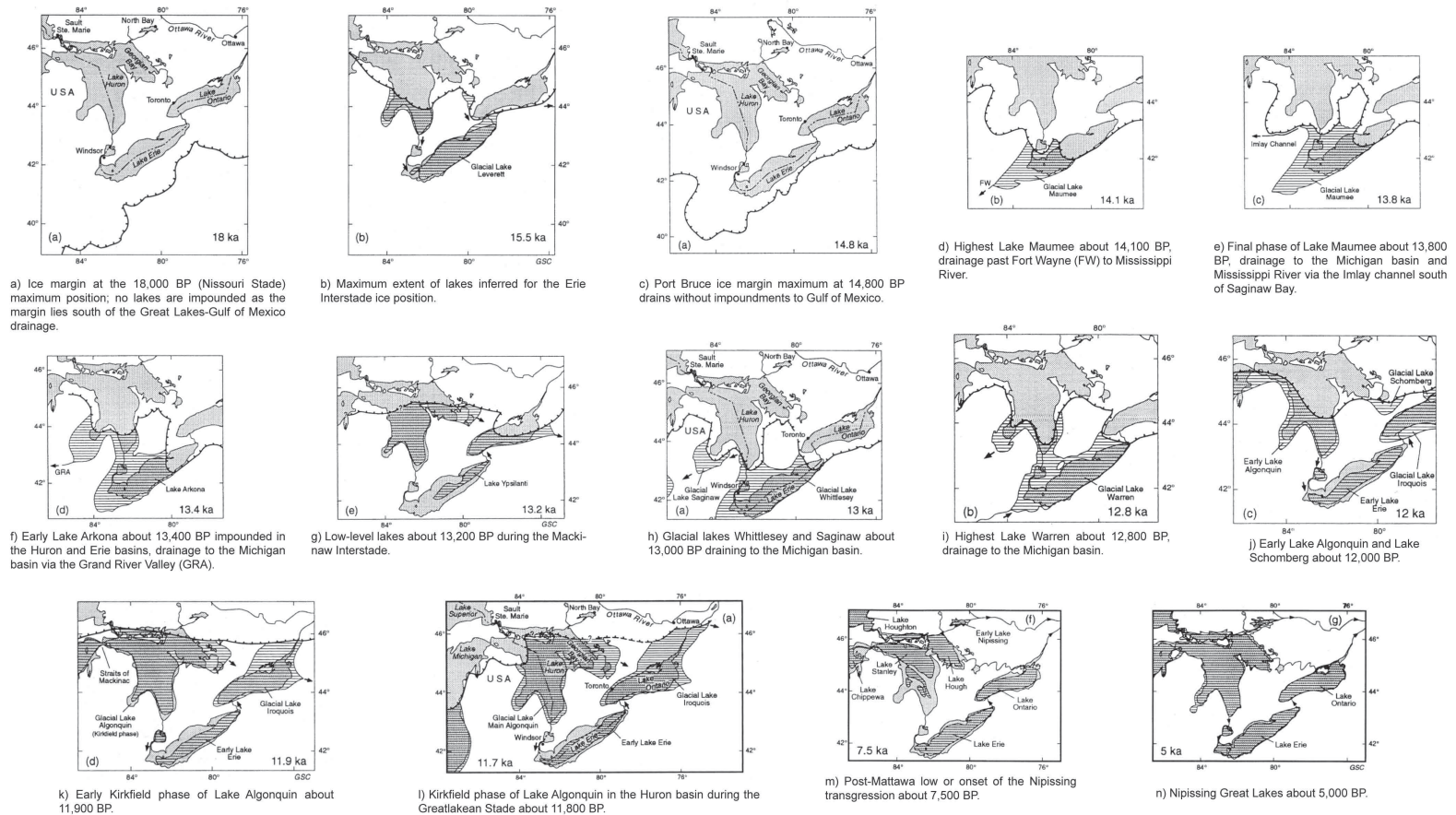
Source: Reference 2.5.1-297

Figure 2.5.1-233 Chart Showing the Lake Phases and Levels and Ice Margin Positions for the Quaternary



Source: Reference 2.5.1-297

Figure 2.5.1-234 Maps Showing Late Wisconsinan Ice Margins and Proglacial Lake Shorelines (~18 ka to 5ka)



Source: Reference 2.5.1-272

Figure 2.5.1-235 Site Exploration Plan

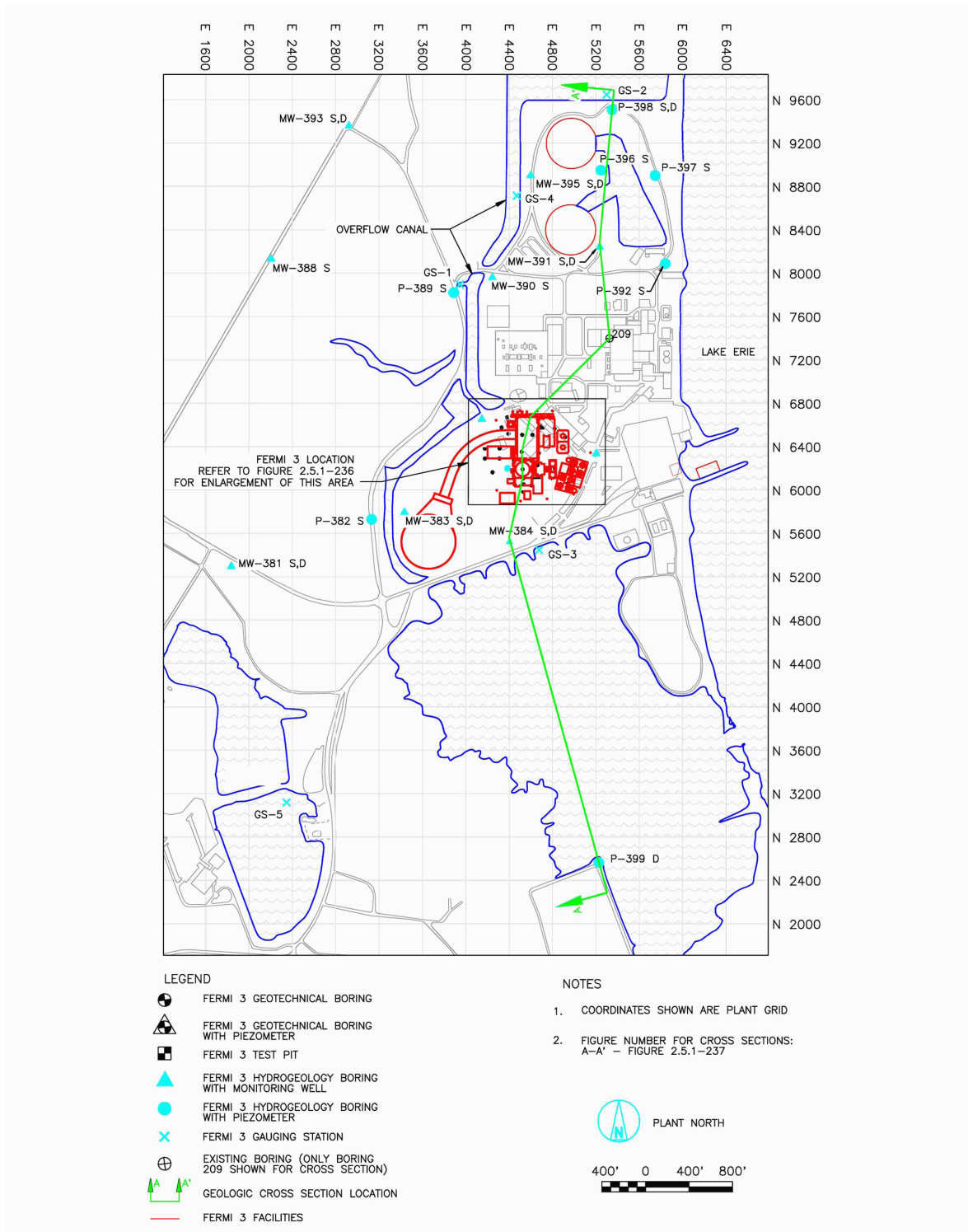


Figure 2.5.1-236 Enlargement of Site Exploration Plan

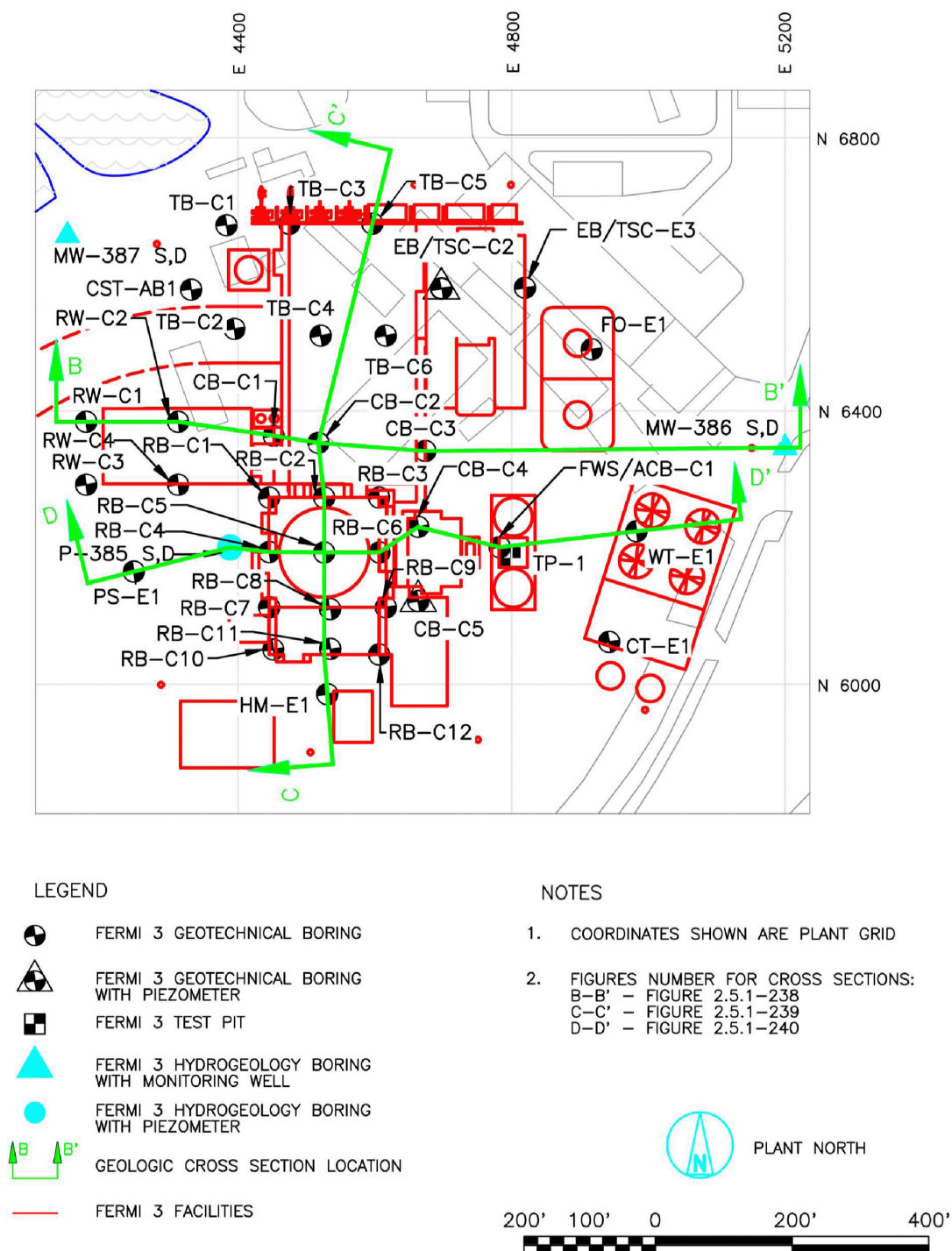


Figure 2.5.1-237 Geologic Cross Section A-A

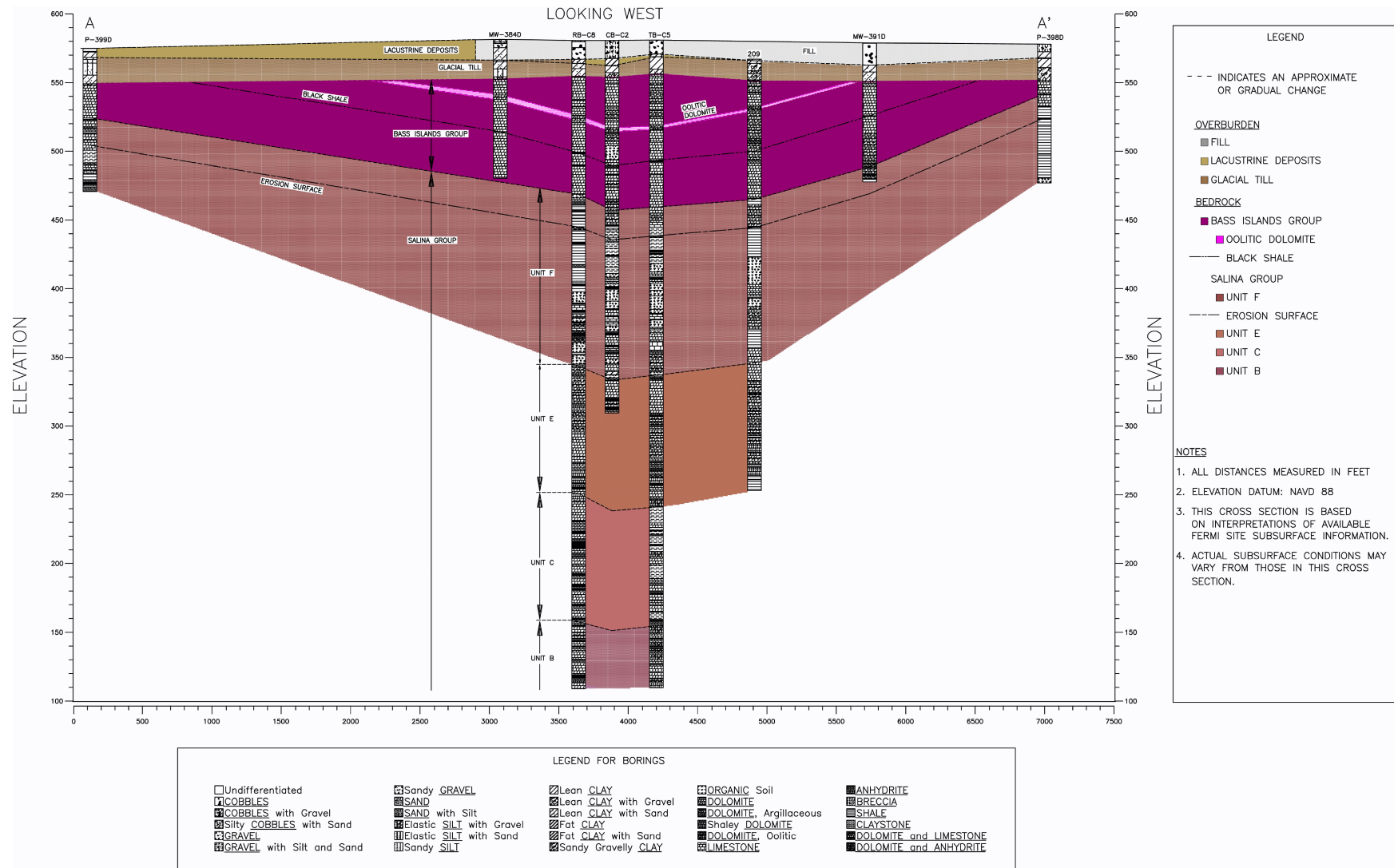


Figure 2.5.1-238 Geologic Cross Section B-B

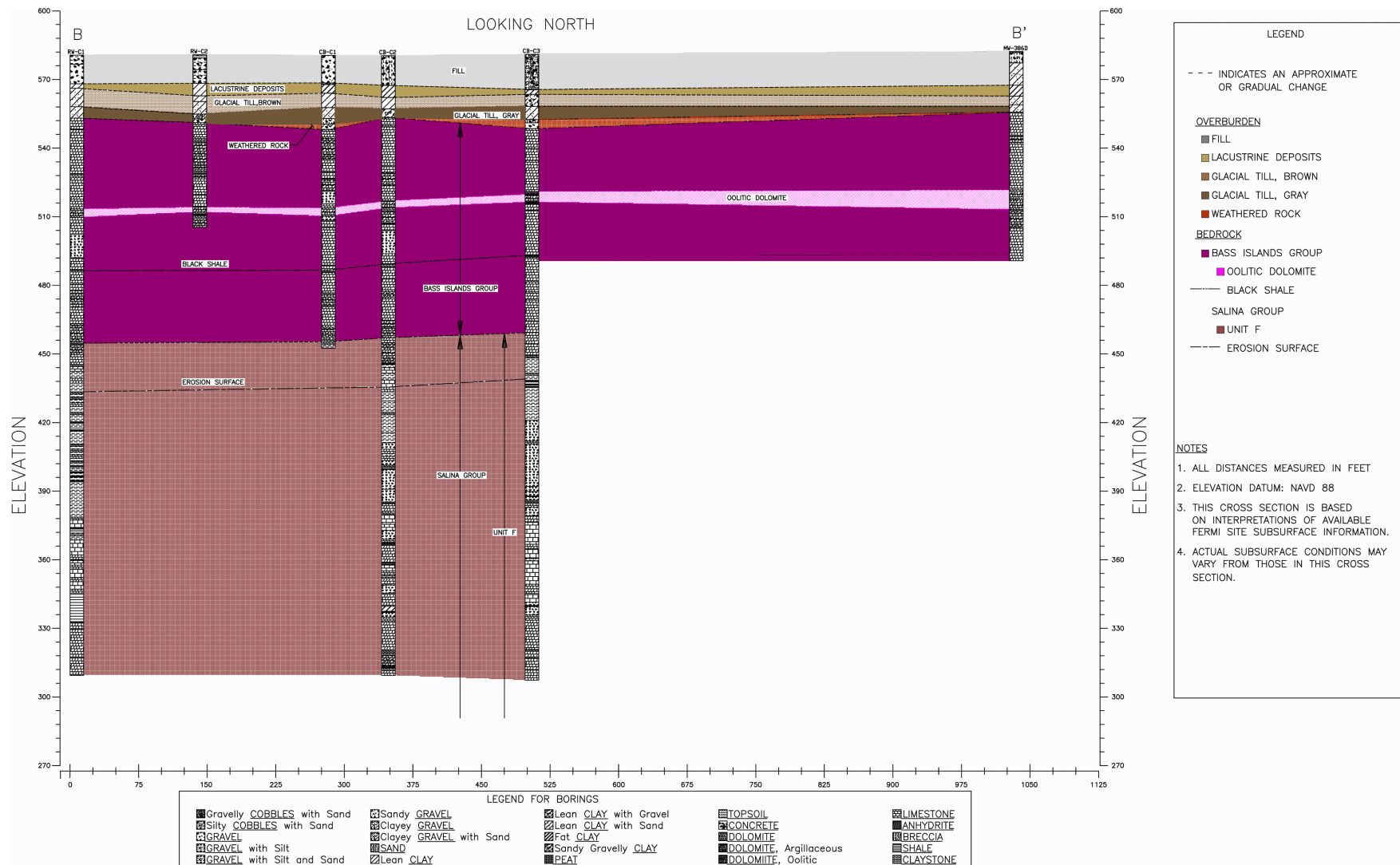


Figure 2.5.1-239 Geologic Cross Section C-C

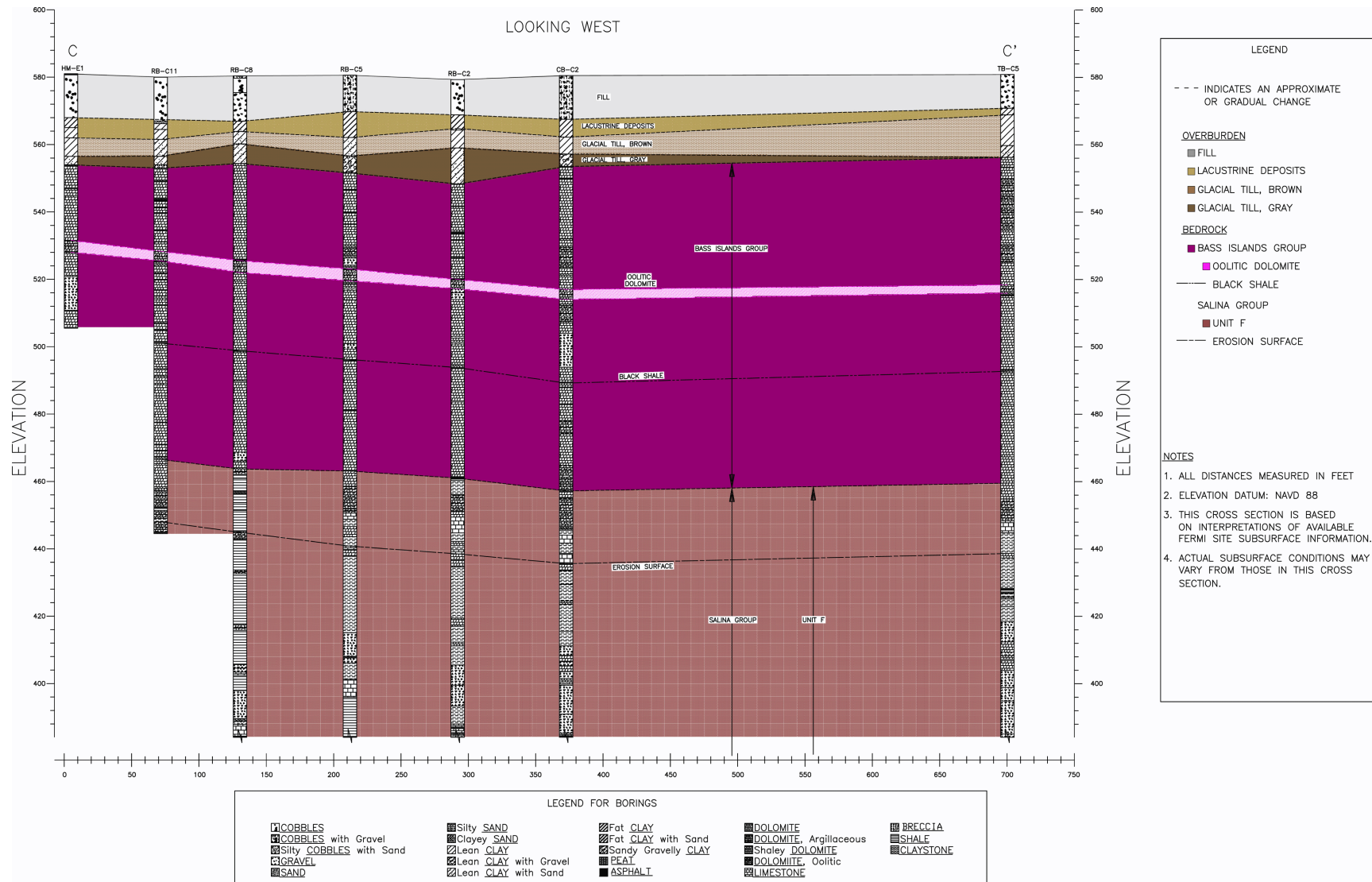


Figure 2.5.1-240 Geologic Cross Section D-D

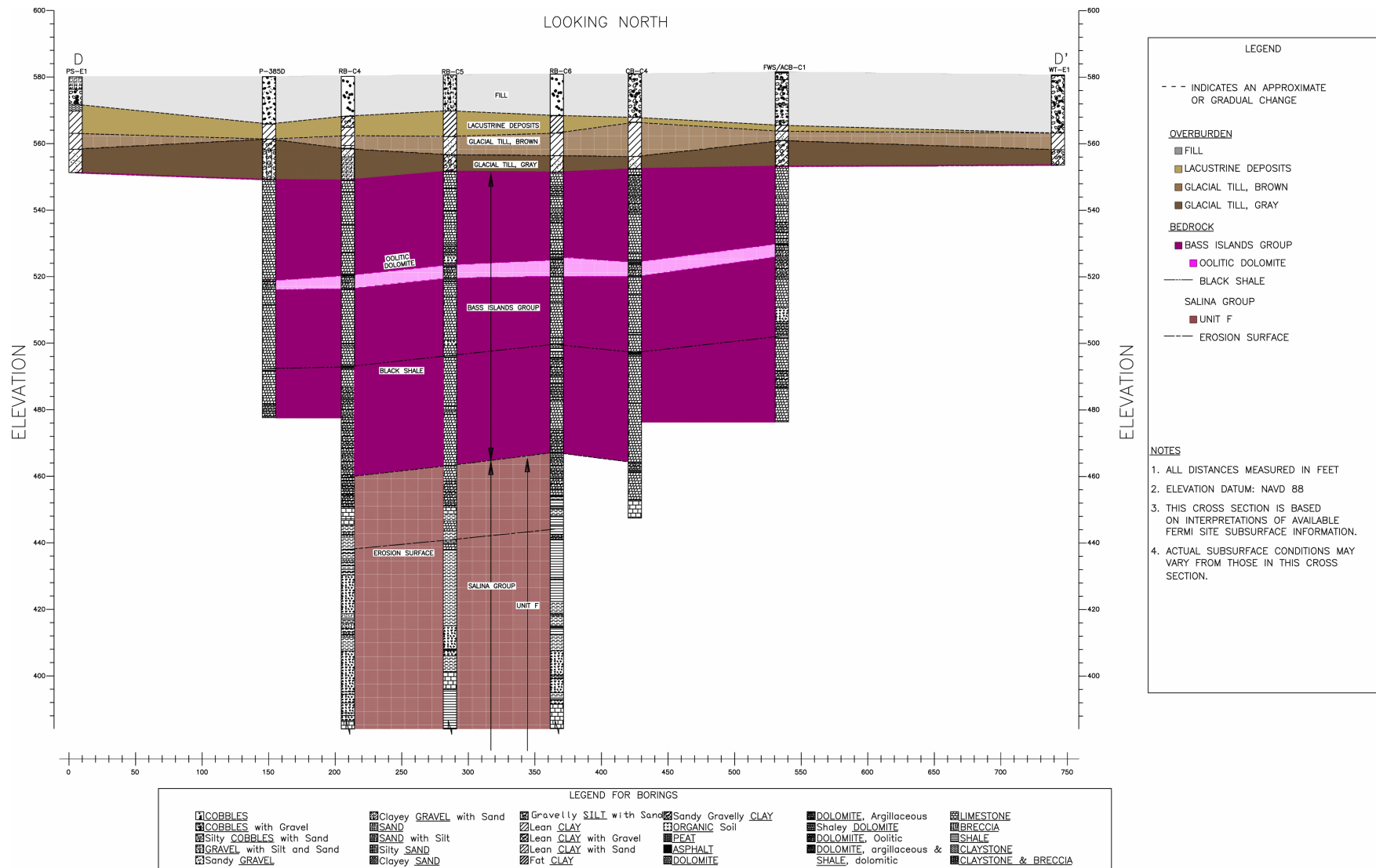


Figure 2.5.1-241 Geologic Map of the Fermi 3 Site Area

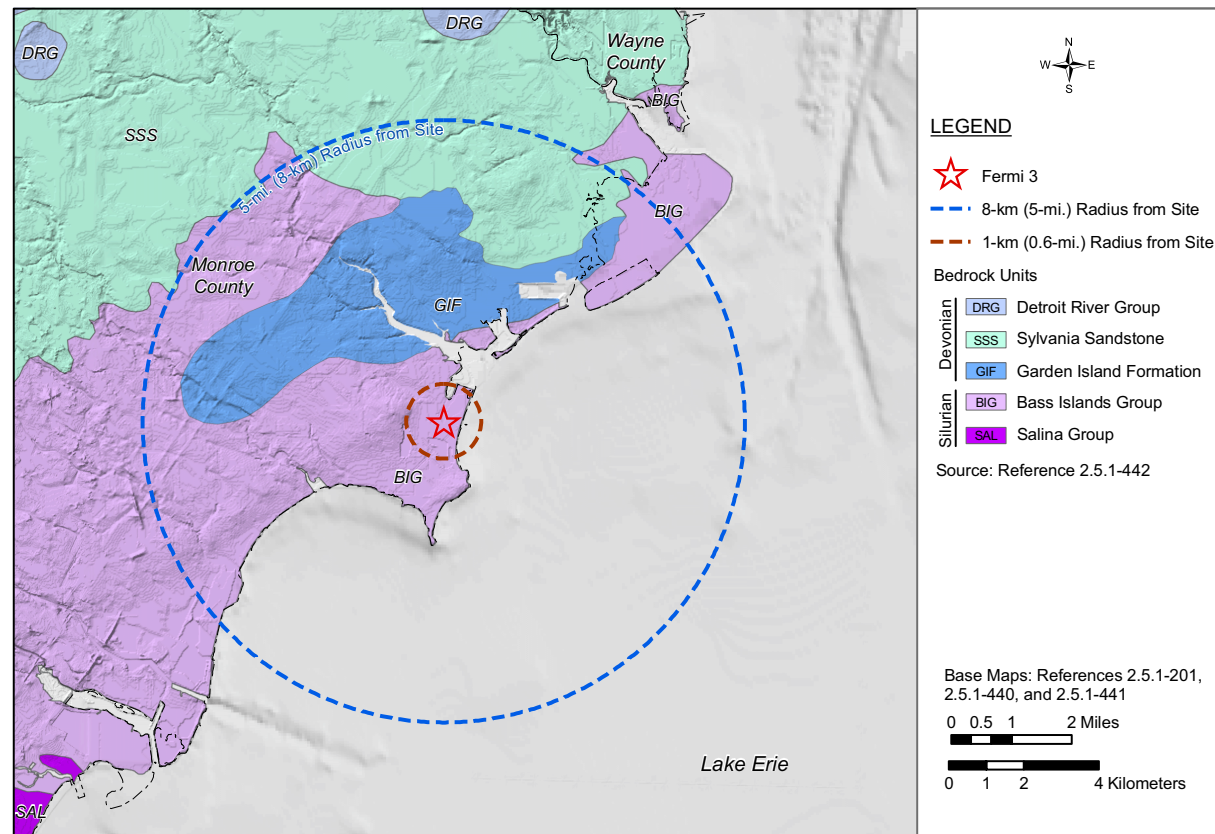


Figure 2.5.1-242 Natural Gamma Log of Fermi 3 Boring RB-C8

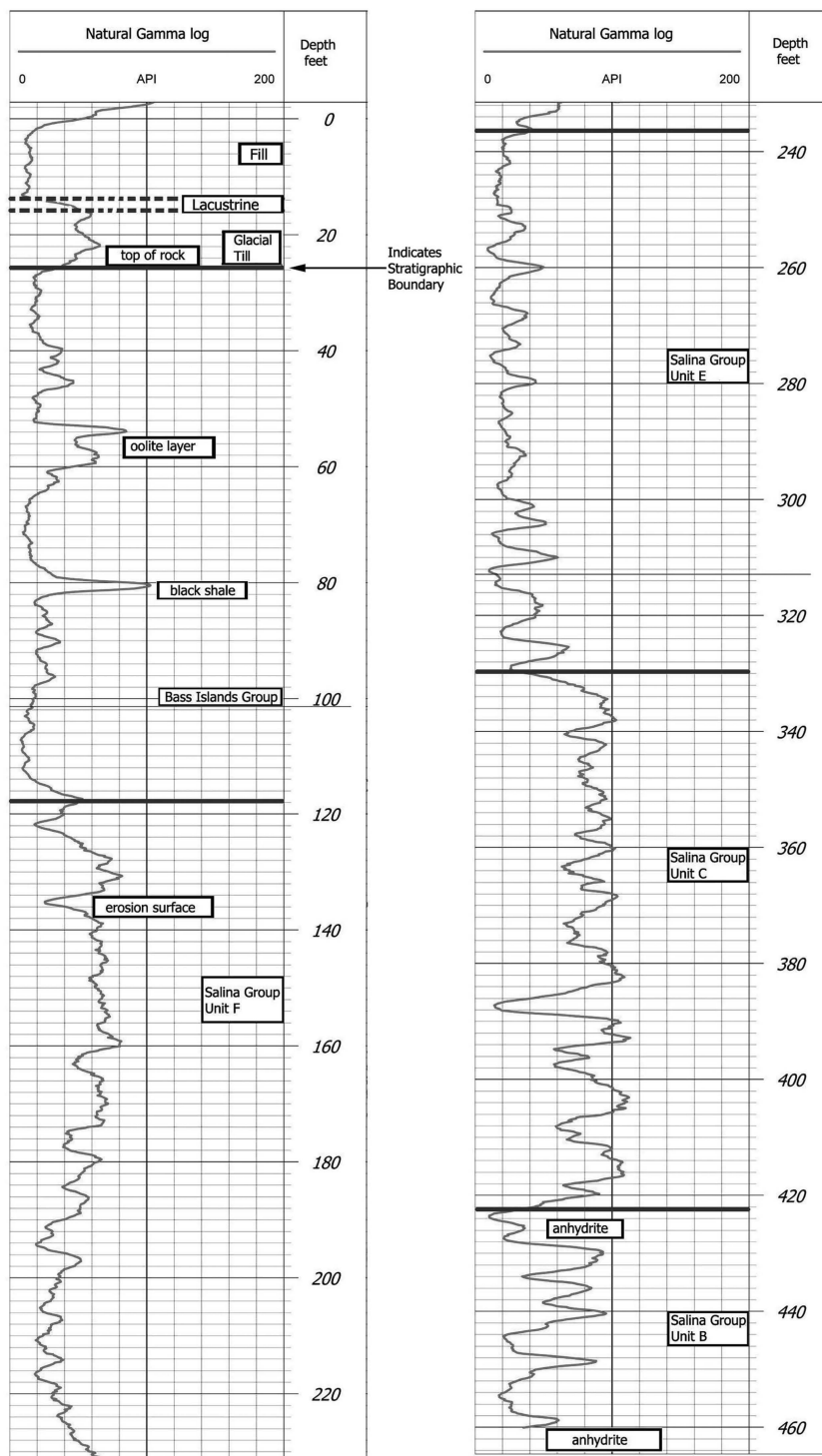


Figure 2.5.1-243 Photograph of Erosion Surface in Salina Unit F, Fermi 3 Boring CB-C2

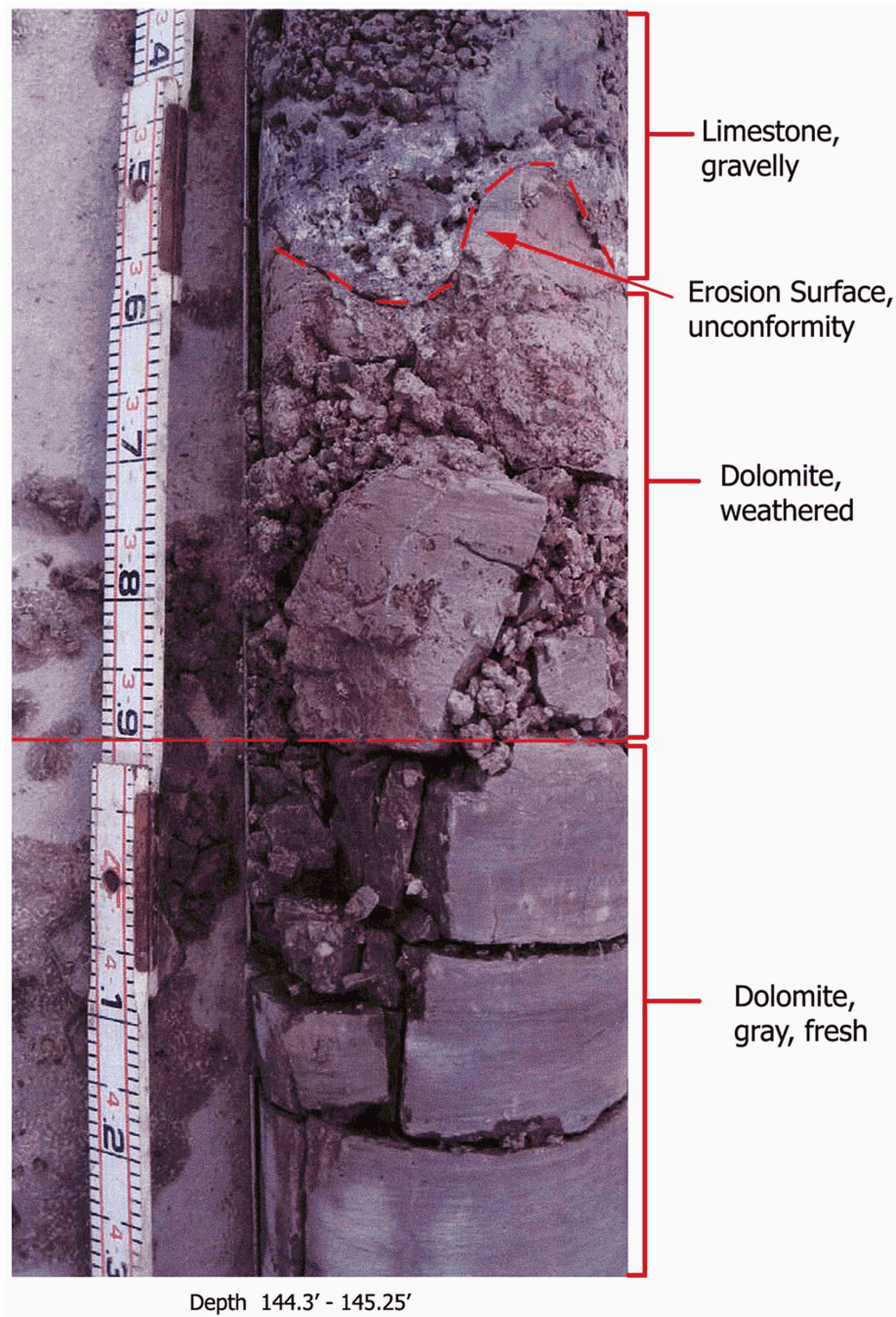


Figure 2.5.1-244 Quaternary Geologic Map of the Site Area

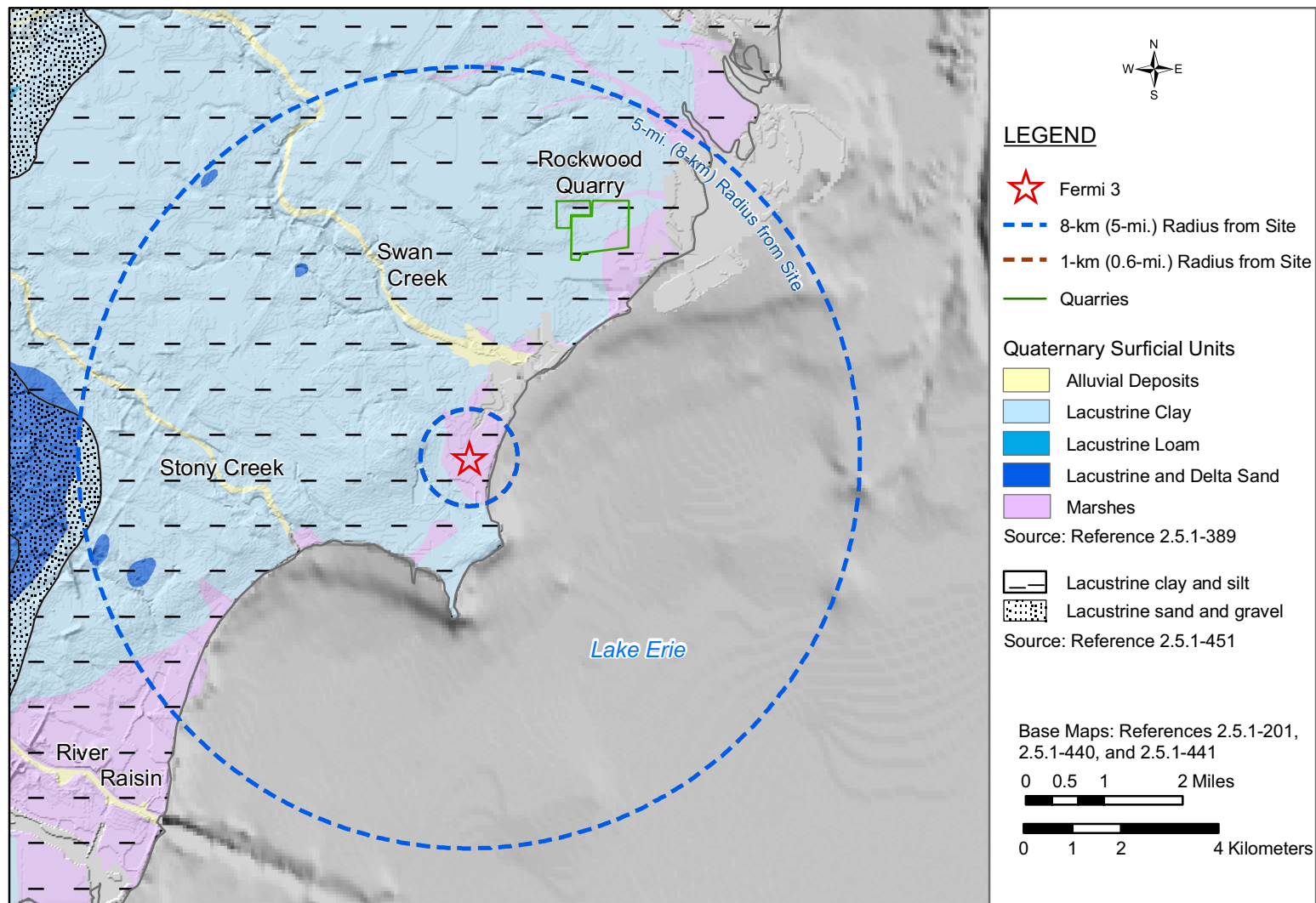


Figure 2.5.1-245 Map Showing Soils of the Fermi 3 Site Location



Figure 2.5.1-246 Tectonic Structures in the Fermi 3 Site Vicinity

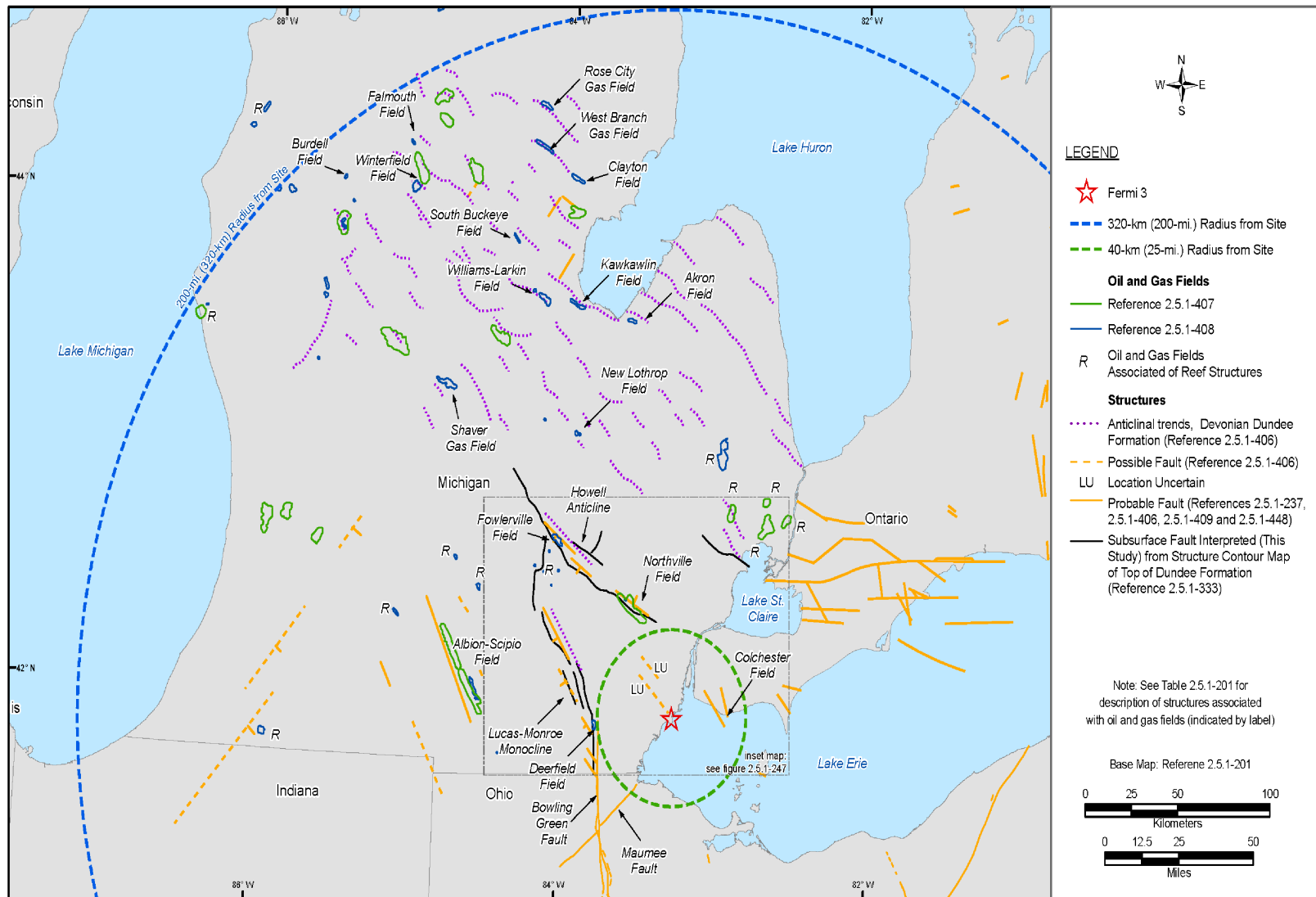


Figure 2.5.1-247 Structure Contour Maps from Monroe County, Michigan

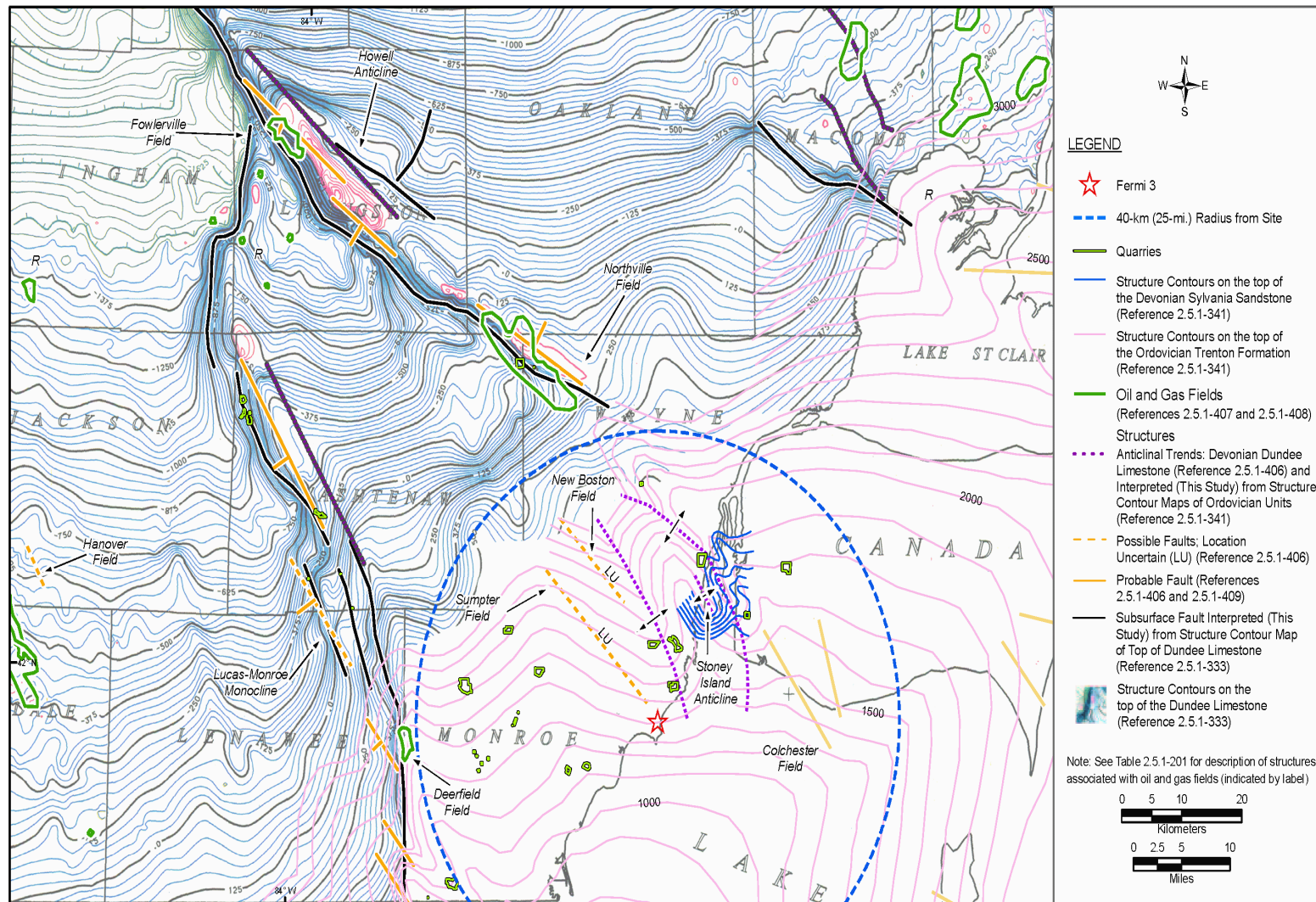
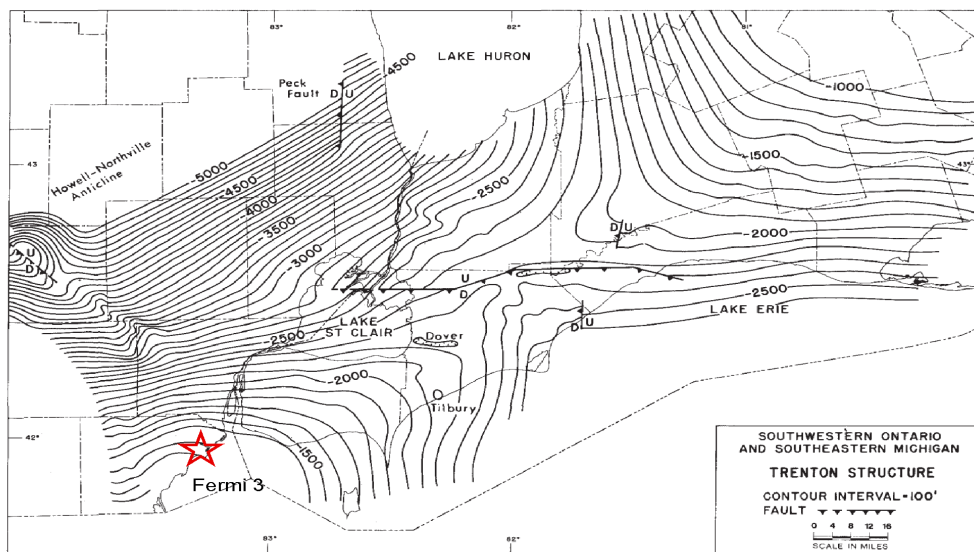
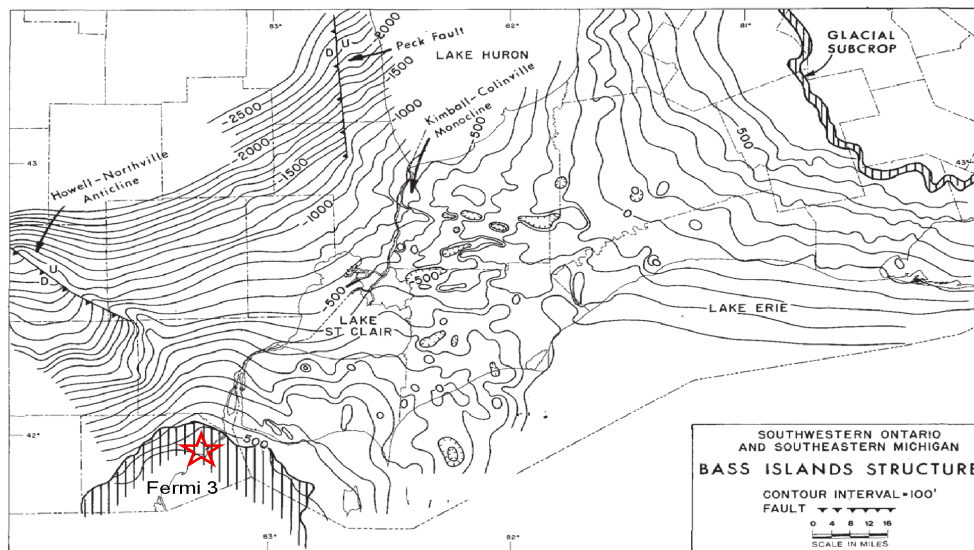


Figure 2.5.1-248 Structural Contour Maps Showing Bedrock Elevation of the Ordovician Trenton Group and the Silurian Bass Islands Formation



a. Structure contour on Ordovician Trenton Group



b. Structure contours on Silurian Bass Islands Formation

Source: Reference 2.5.1-325

Figure 2.5.1-249 Structural Contour Map on the Top of the Bass Islands Group, Oolitic Dolomite Marker Horizon

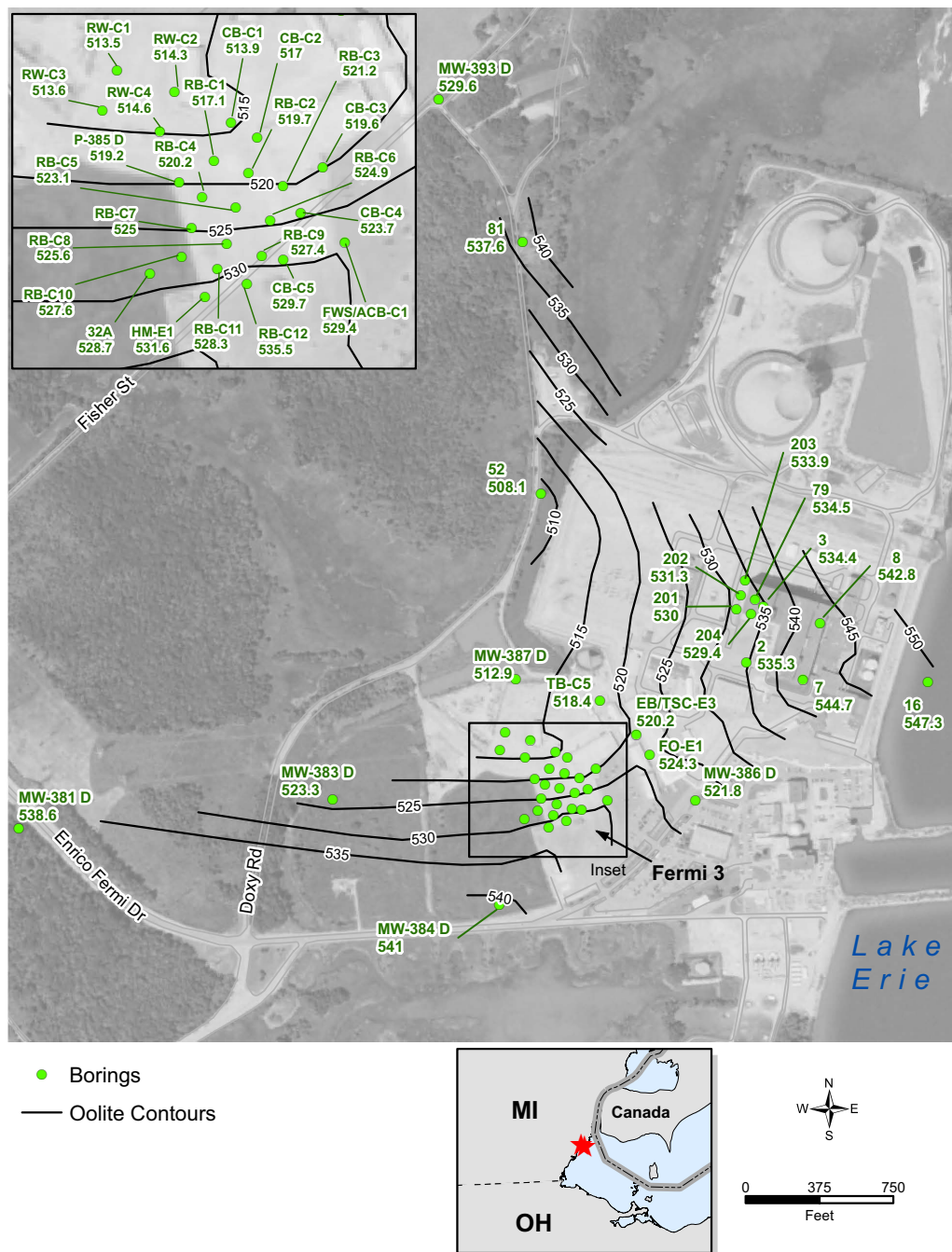


Figure 2.5.1-250 Fermi 3 Site Vicinity Physiographic Map

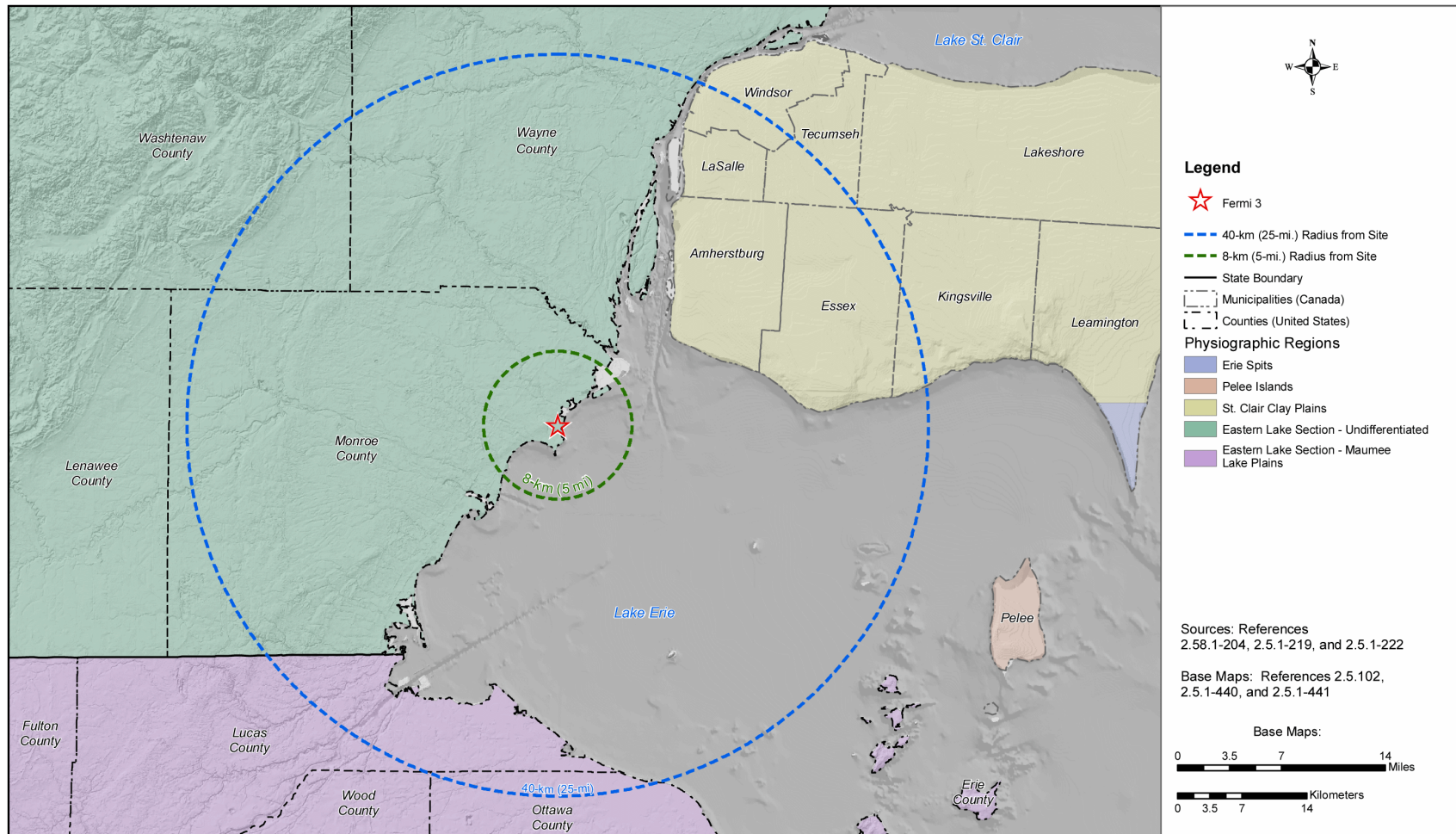
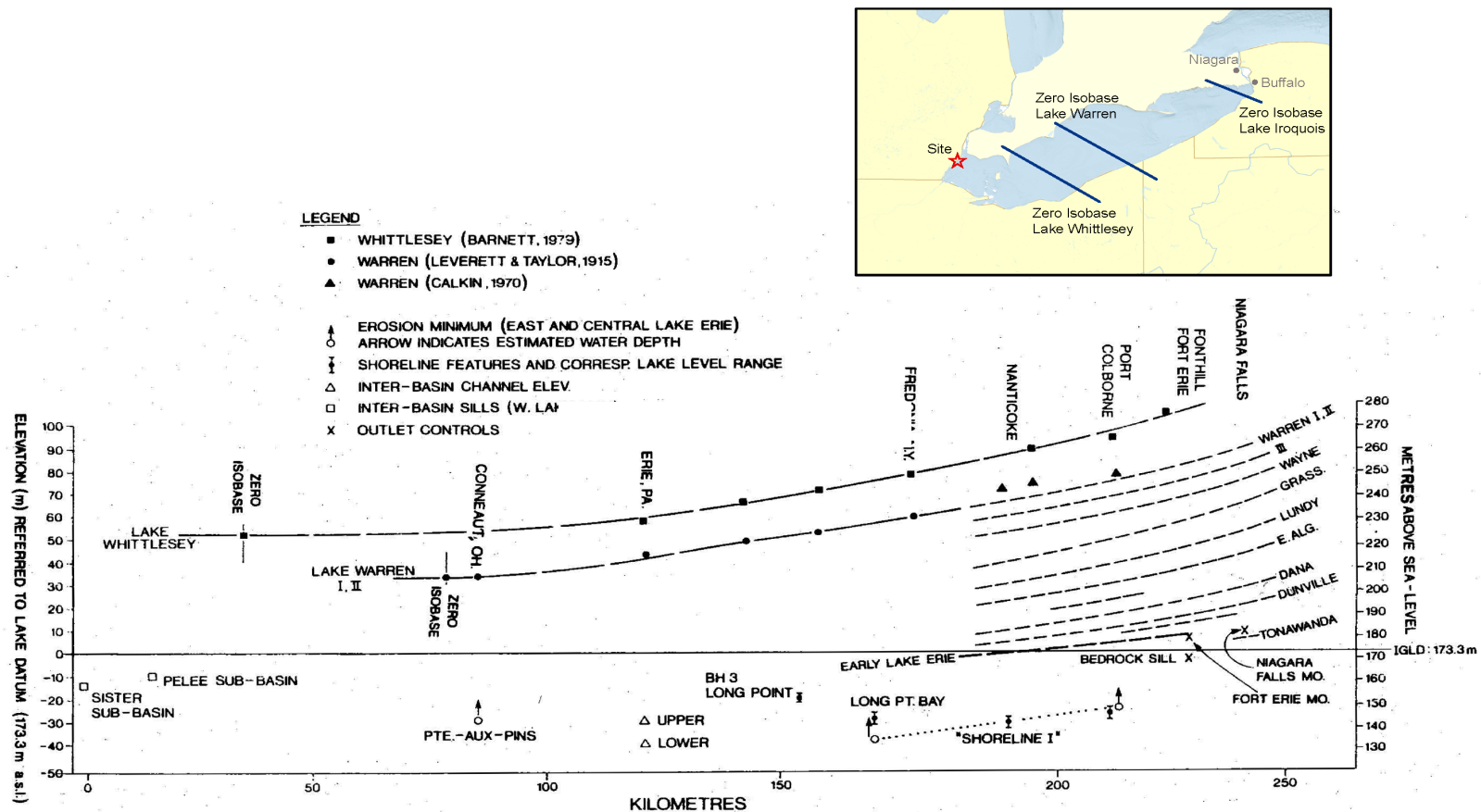


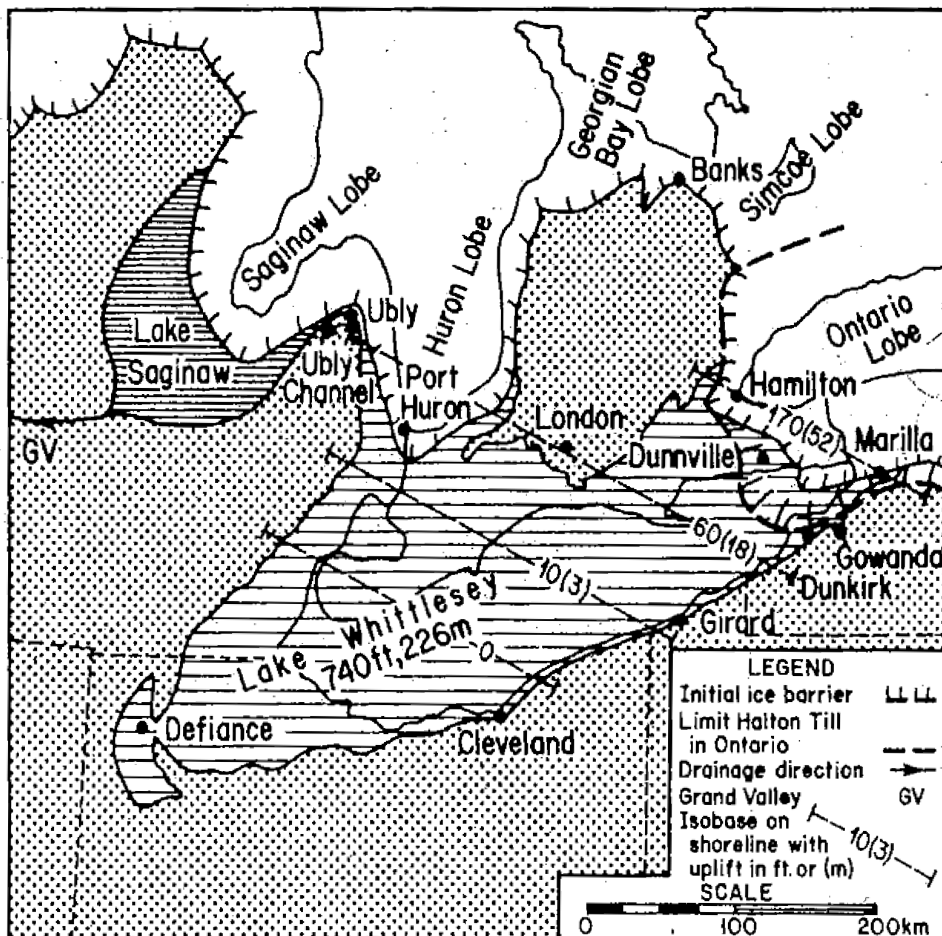
Figure 2.5.1-251 Plot of Elevation Versus Distance of Raised and Uptilted Shorelines of the Whittlesey and Subsequent Lake Phases



Note. Profile is oriented N 24° E, the direction of maximum tilting. Also plotted are submerged geomorphological features noted on or below the lake bottom, and their relationship to possible outlet controls at the Niagara River.

Source: Reference 2.5.1-296

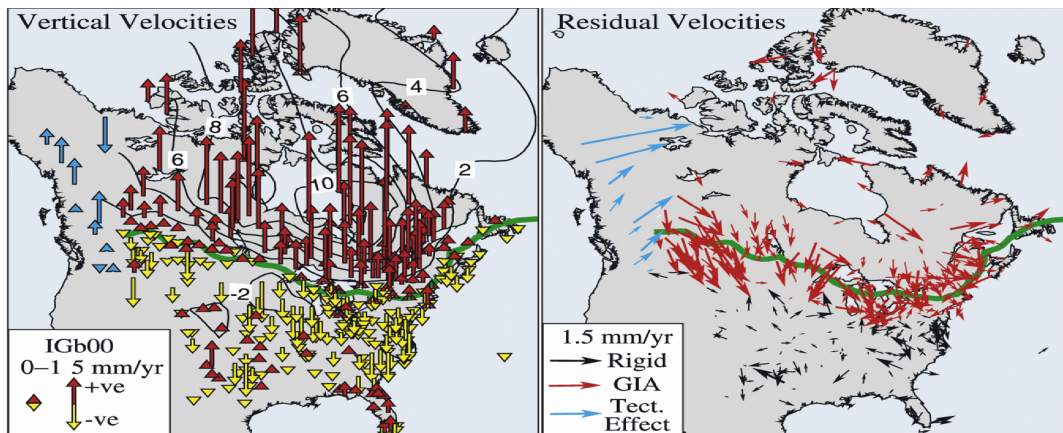
Figure 2.5.1-252 Lakes Whittlesey and Saginaw, and the Port Huron Stade Ice Barriers



Note. Isobases on Whittlesey shoreline features tilted in N27°E direction. The true isobases may bow southwestward more nearly parallel to former ice margins as they cross the basin.

Source: Reference 2.5.1-297

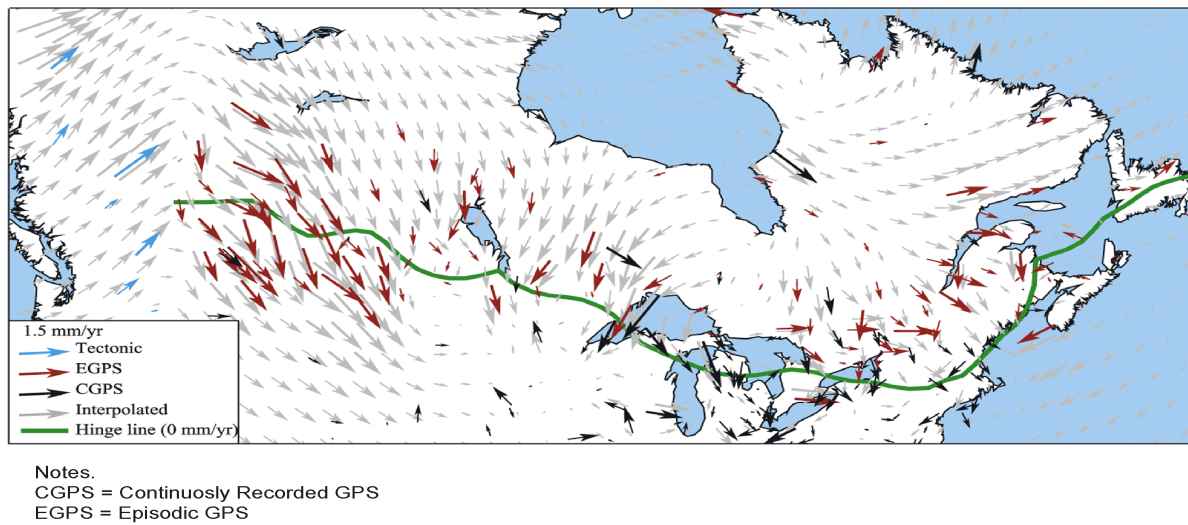
Figure 2.5.1-253 GPS Motions



Note. (left) Vertical GPS site motions with respect to IGB00. Note large uplift rates around Hudson Bay, and subsidence to the south. Green line shows interpolated 0 mm/yr vertical "hinge line" separating uplift from subsidence. (right) Horizontal motion site residuals after subtracting best fit rigid plate rotation model defined by sites shown with black arrows. Red vectors represent sites primarily affected by GIA. Blue vectors represent sites that include effects of tectonics.

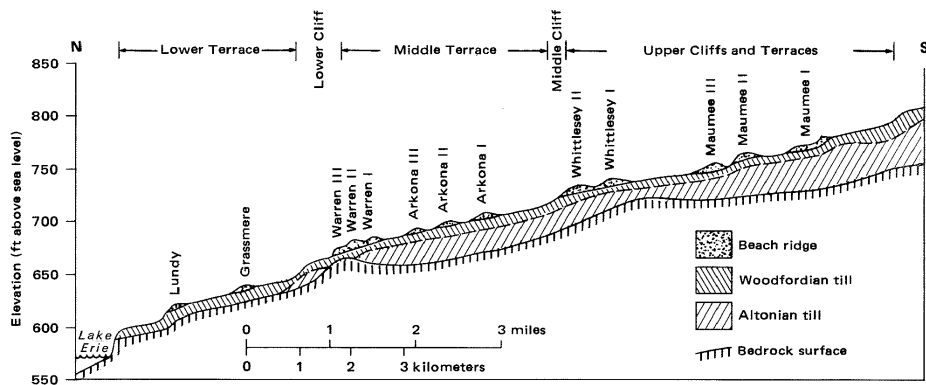
Source: Reference 2.5.1-291

Figure 2.5.1-254 GPS Horizontal Velocities with Motion of Rigid North America Removed

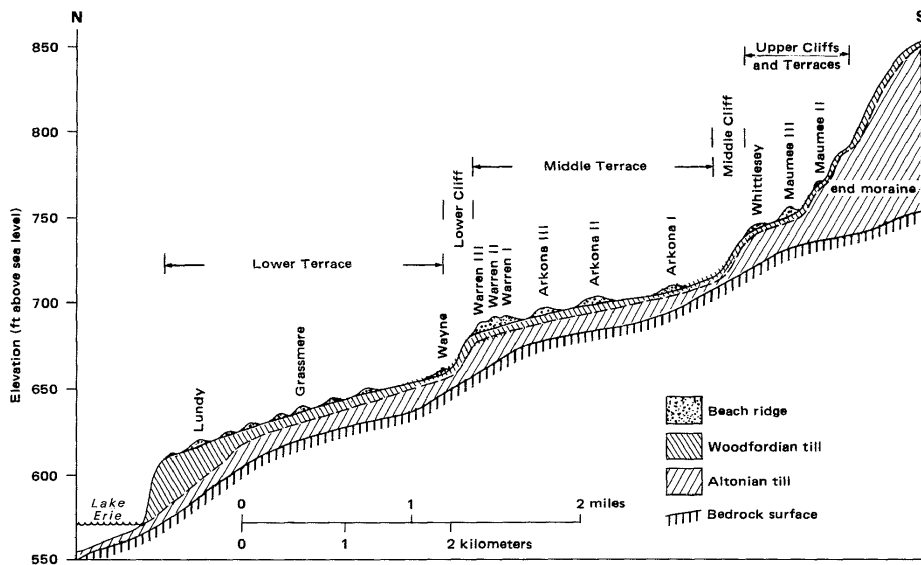


Source: Reference 2.5.1-291

Figure 2.5.1-255 Composite Cross Sections of Strandlines in Northern Ohio



Composite cross section of strandlines south of Lake Erie in Lorain and western Cuyahoga Counties.



Composite cross section of strandlines south of Lake Erie in Lake and Ashtabula Counties.

Note. Three features are evident: (1) cliffs and terraces cut into bedrock; (2) cliffs and terraces cut into Altonian till (early Wisconsinian in age) and later mantled with Woodfordian till (late Wisconsinian in age); and (3) beach ridges on terraces.

Source: Reference 2.5.1-489

Figure 2.5.1-256 Paleo-shorelines and Structural Features in the Vicinity of Fermi 3 Site

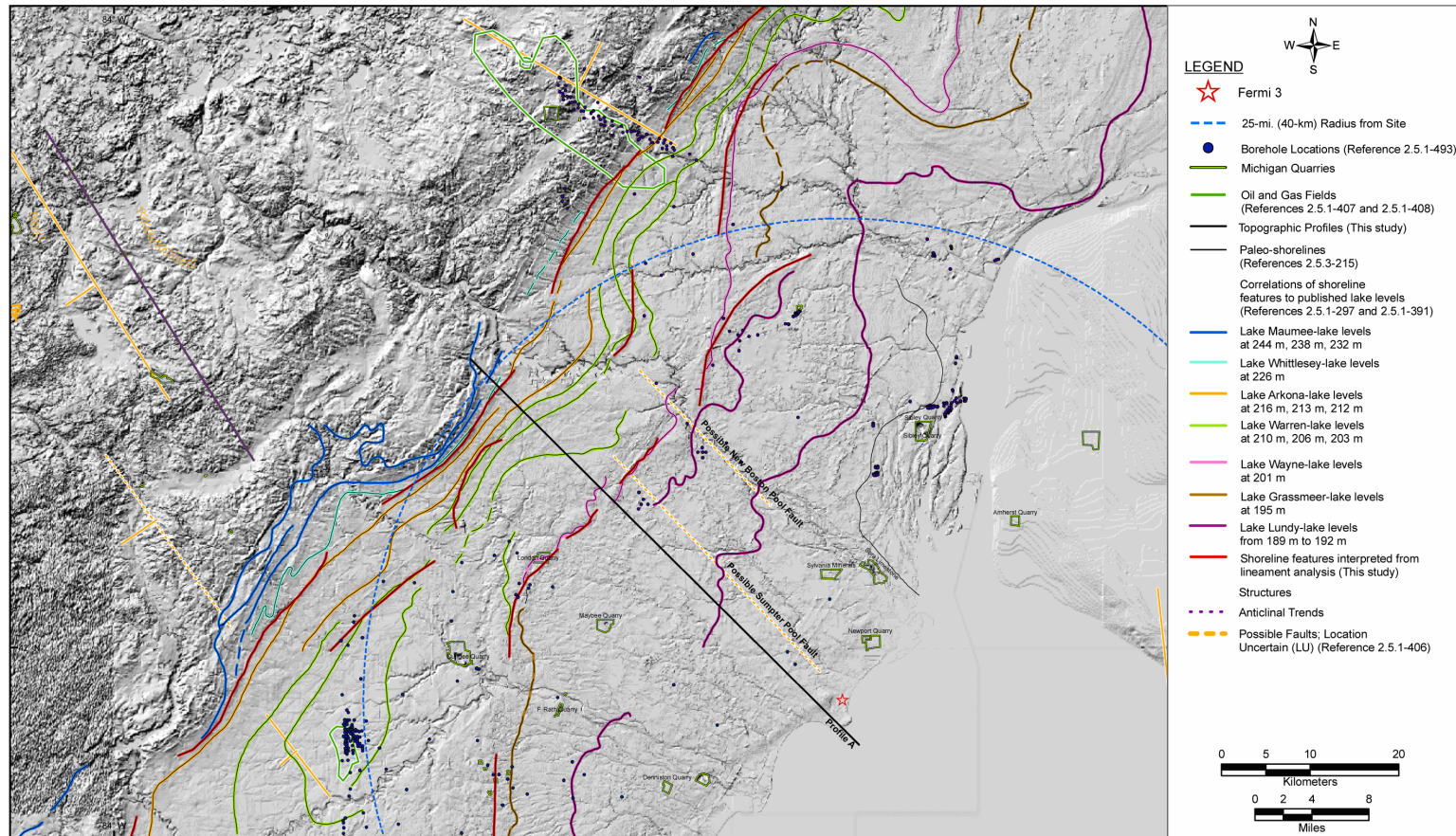
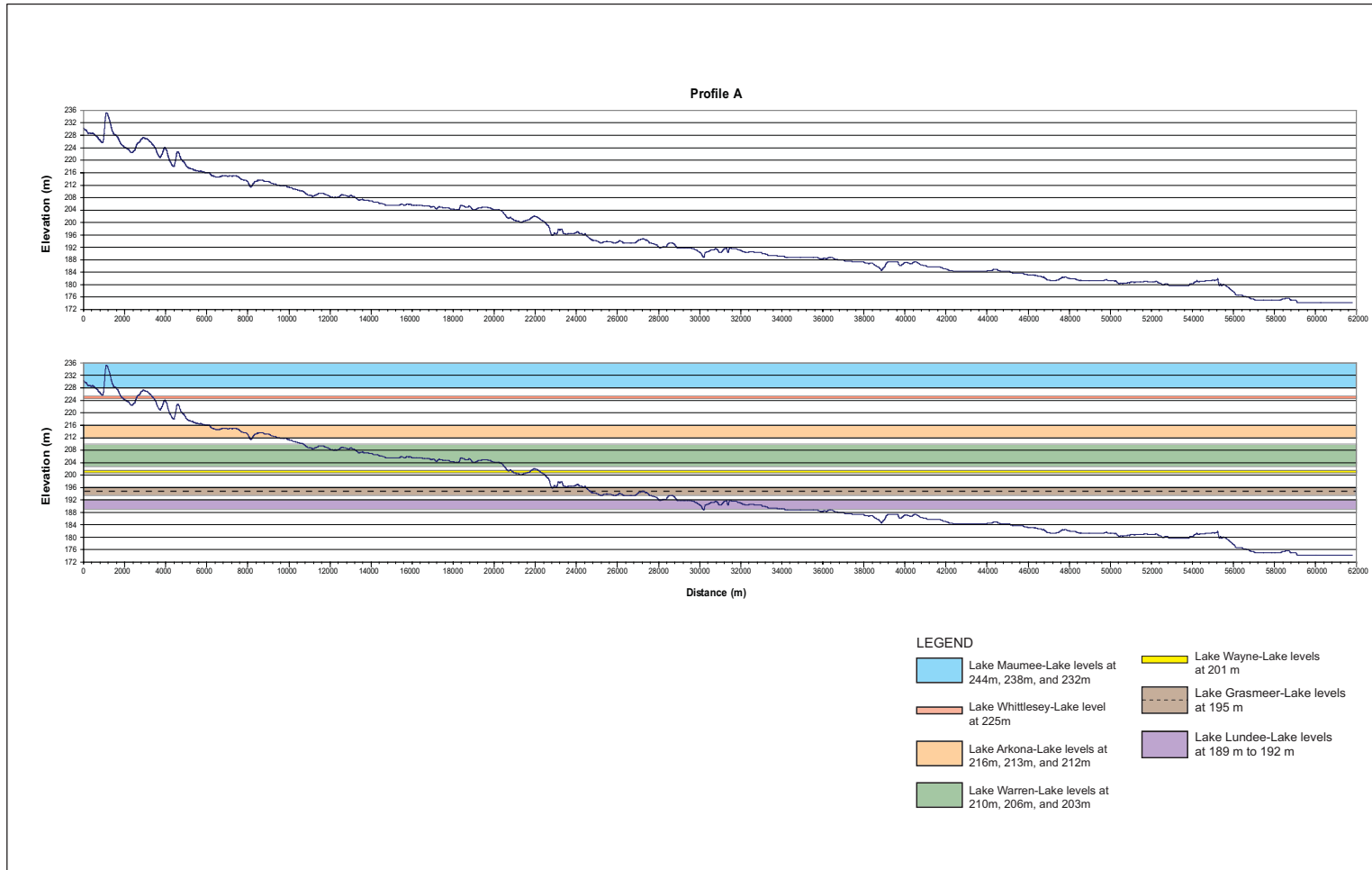


Figure 2.5.1-257 Topographic Profile AA' Relative to Published Elevations of Mapped Paleo-shoreline Features



Source: Reference 2.5.1-497, Reference 2.5.1-391

Figure 2.5.1-258 Denniston Quarry: Quaternary Excavations, Soil Profile Locations and Mapped Soil Units



Figure 2.5.1-259 Denniston Quarry: Soil Profile SP-1 in Quaternary Excavation QE-1



Photograph showing SP-1 soil horizon boundaries (designated by depth).

Figure 2.5.1-260 Denniston Quarry: Stratigraphy Exposed in Quaternary QE-2

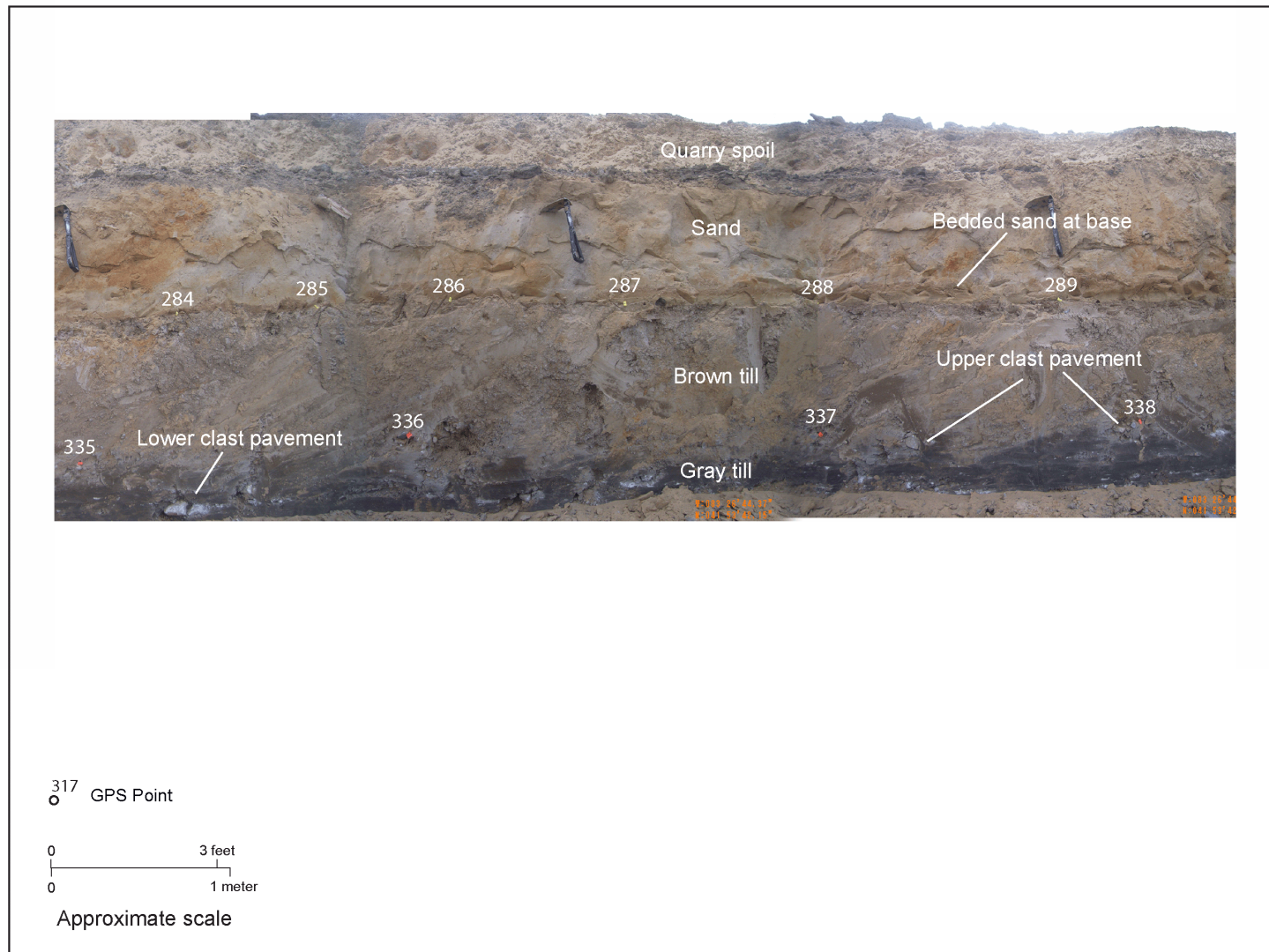
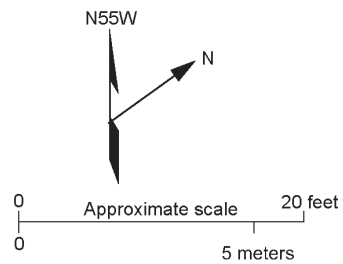
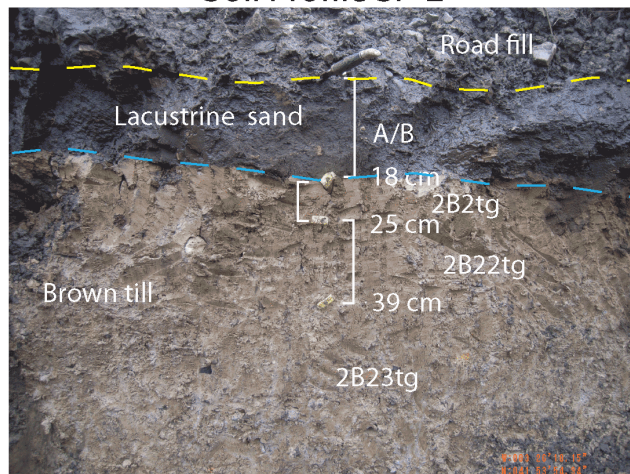


Figure 2.5.1-261 Denniston Quarry: Quaternary Excavation QE-3 and Soil Profiles SP-2 and SP-3



Soil Profile SP-2



Soil Profile SP-3

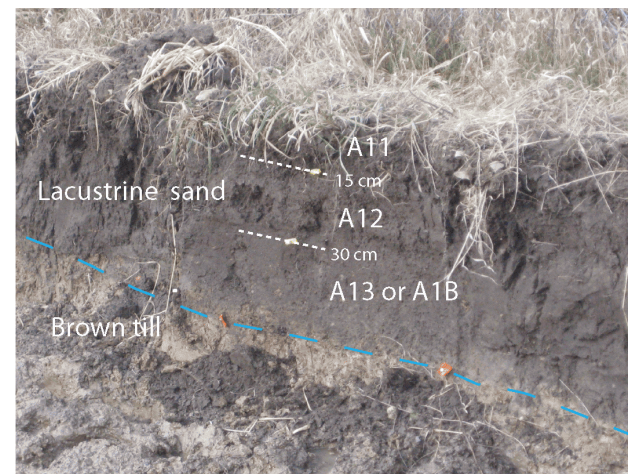
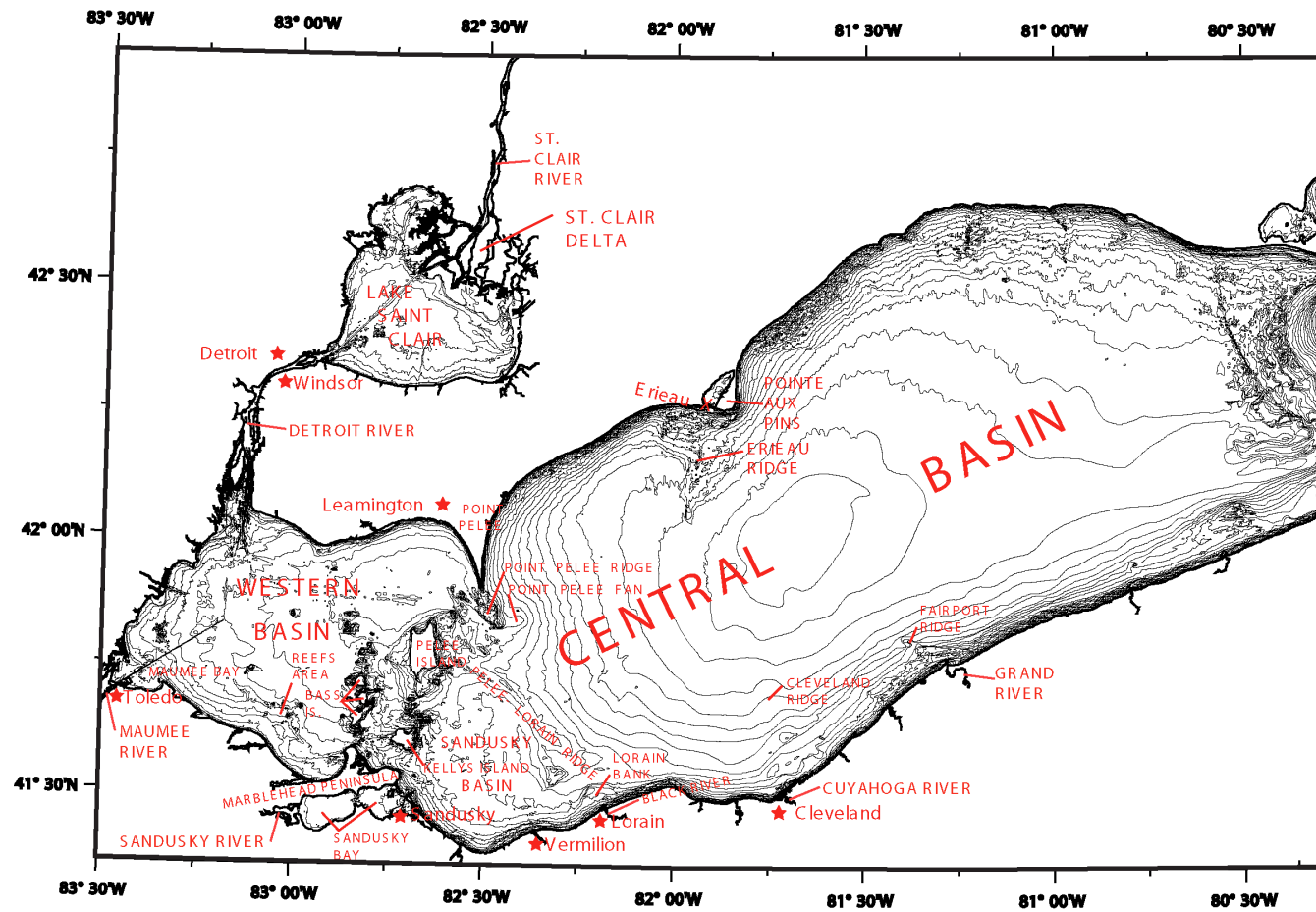


Figure 2.5.1-262 Denniston Quarry: North Wall of Quaternary Excavation QE-3

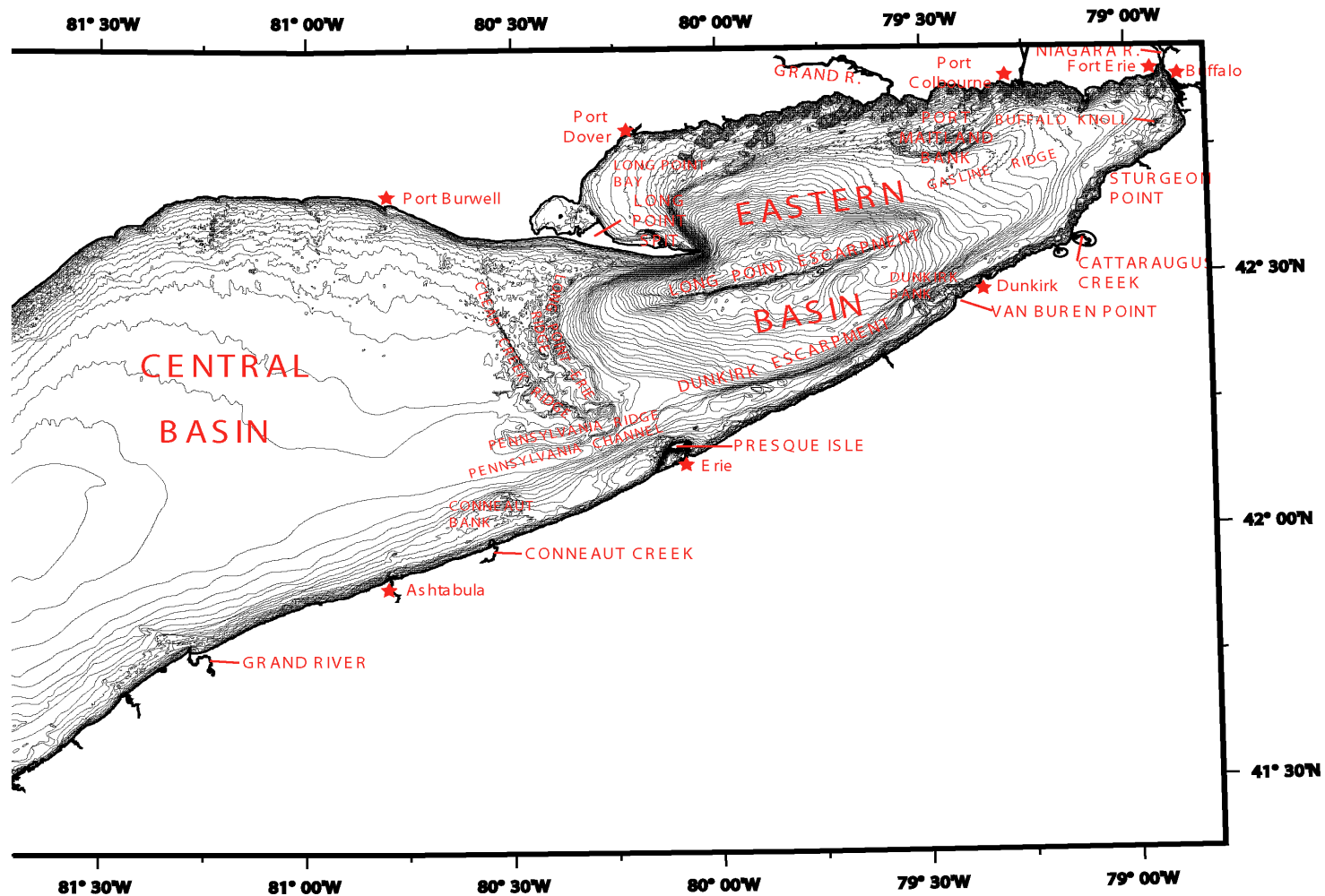


Figure 2.5.1-263 Index Map of Western Lake Erie Showing Names of Geographic Features



Source: Reference 2.5.1-494

Figure 2.5.1-264 Index Map of Eastern Lake Erie Showing Names of Geographic Features



Source: [Reference 2.5.1-494](#)

Fermi 3
Updated Final Safety Analysis Report

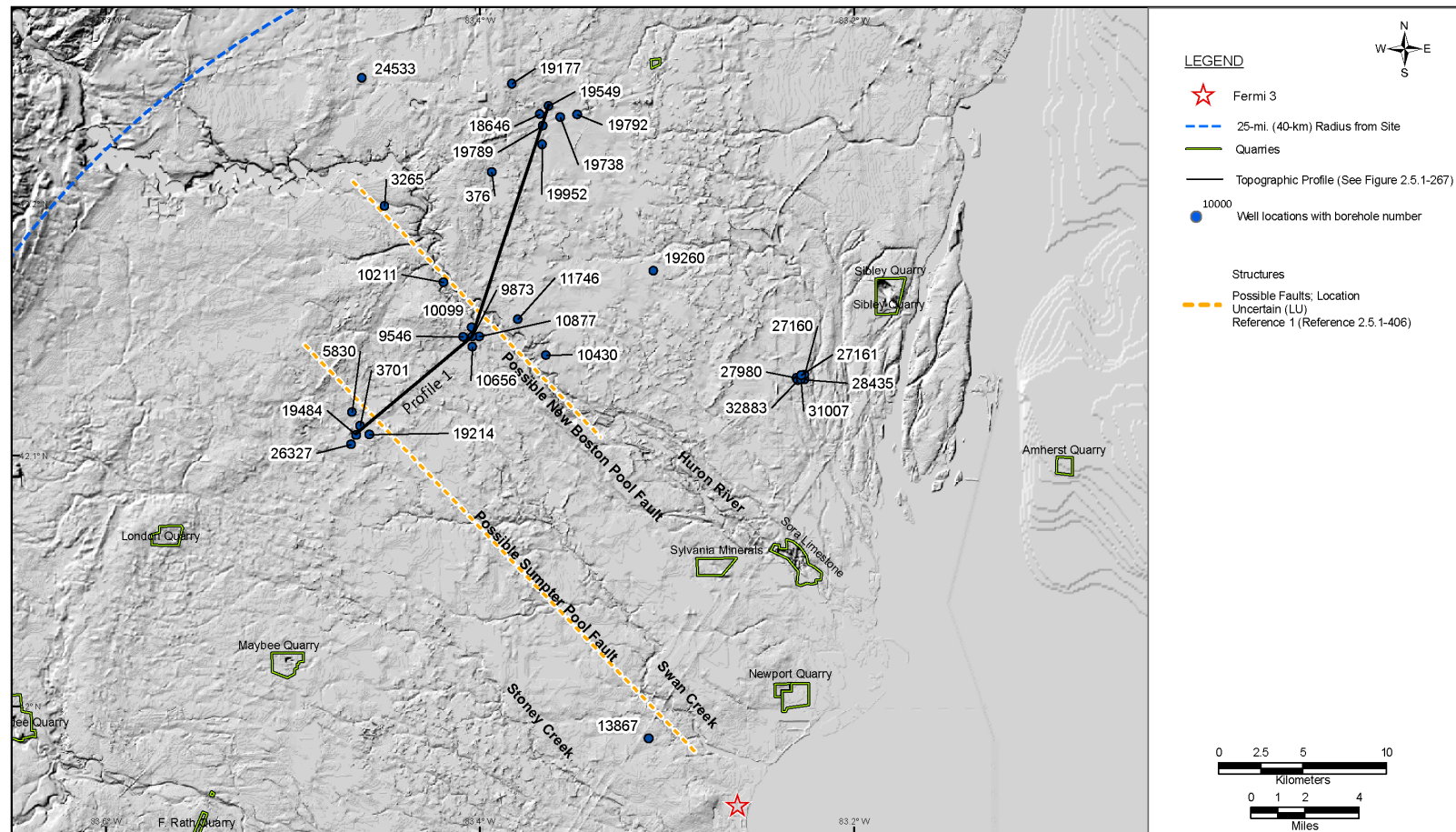
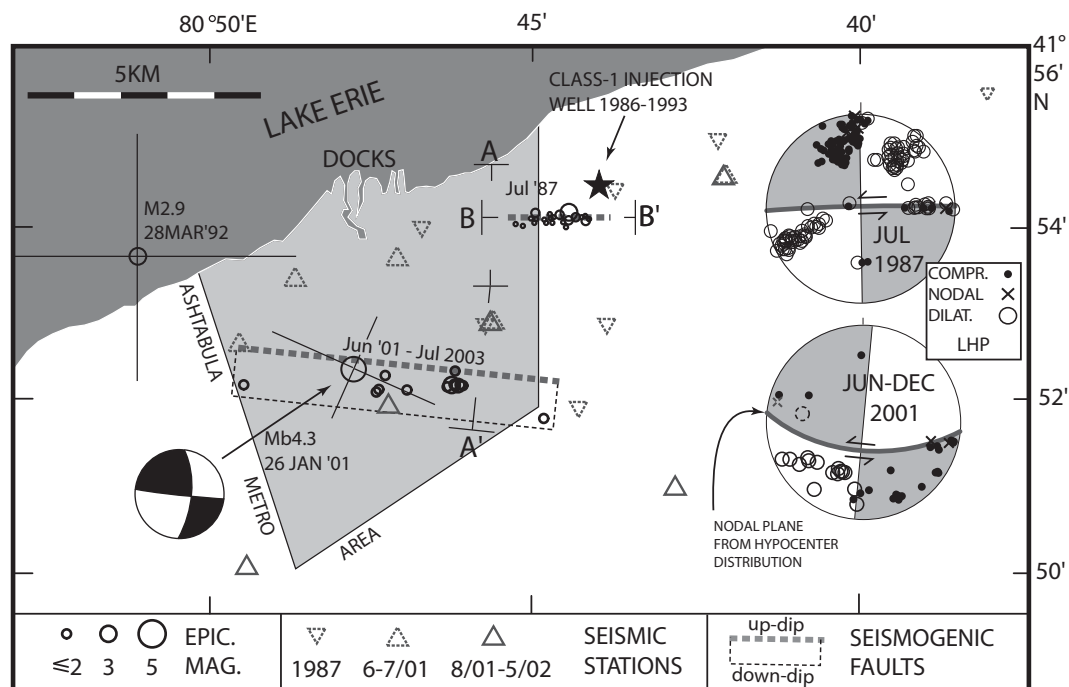


Figure 2.5.1-266 Earthquake and Inferred Fault Planes in the Ashtabula, Ohio, Area

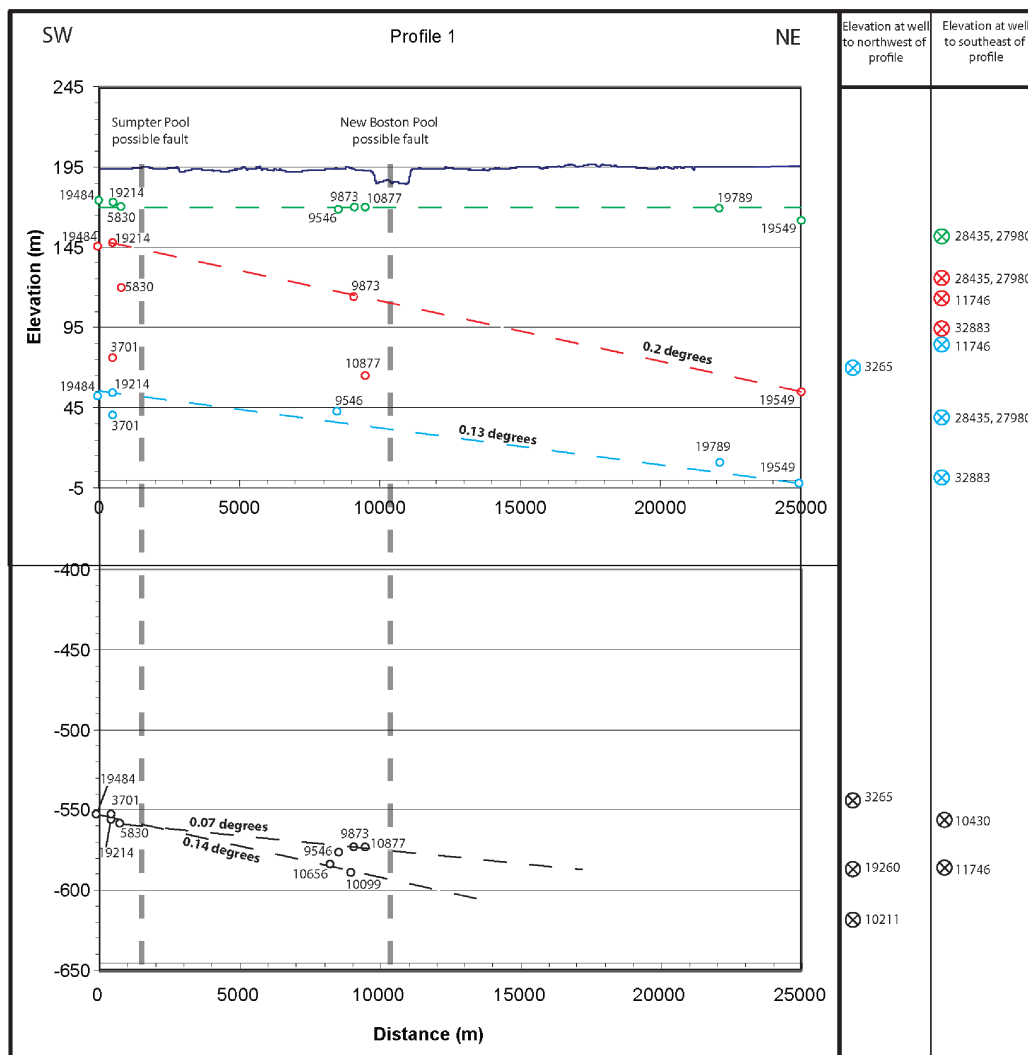


Reference 2.5.1-455

Accurate hypocenters and first motions in Ashtabula, Ohio, from two short-term deployments of portable seismographs. Data from 1987 illuminated a vertical east-west-striking left-lateral fault in the basement (Seeber and Armbruster, 1993). This activity was 0.7–2.0 km from a waste-disposal well (star) and started 1 year after the onset of injection. Several episodes of felt earthquakes during the following years were not monitored by local instruments. An M_{blg} 4.3 mainshock on 26 January 2001 caused light damage (MMI VI). The focal mechanism (Du *et al.*, 2003) and epicenter of this event were obtained from regional waveforms. Another fore–main–aftershock subsequence during June 2001 was captured with a local network. These data illuminate another fault (thick line is fault trace at unconformity) similar to the one in 1987, but 4 km south. The January mainshock is probably also from this source. The two dotted first motions are from the latest and westernmost hypocenter and are inconsistent with the composite focal mechanism.

Reference Reference 2.5.1-455

Figure 2.5.1-267 Plot Showing Elevations of Bedrock Surfaces Based on Oil Wells across the Sumpter Pool and New Boston Pool Possible Faults



LEGEND

- Top of Dundee Formation
- Top of Sylvania Formation
- Top of Bass Islands Group
- Top of Trenton Formation
- Approximate apparent dip based on well elevations
- Well along Profile 1 with well number (See Figure 2.5.1-265 for well locations)
- ⊗ Well in vicinity of Profile 1 with well number (See Figure 2.5.1-265 for well locations)

Note: Locations of possible faults from Reference 1 (Reference 2.5.1-406)